DOE/ET/53088-50 IFSR #50

CURVATURE-DRIVEN INSTABILITIES IN A HOT ELECTRON PLASMA: RADIAL ANALYSIS

H. L. Berk, J. W. Van Dam, M. N. Rosenbluth
Institute for Fusion Studies

and

D. A. Spong
Oak Ridge National Laboratory

December 1981

CURVATURE-DRIVEN INSTABILITIES IN A HOT ELECTRON PLASMA: RADIAL ANALYSIS

H. L. Berk
J. W. Van Dam
M. N. Rosenbluth

Institute for Fusion Studies
University of Texas at Austin
Austin, Texas 78712

and

D. A. Spong
Oak Ridge National Laboratory
Oak Ridge, Tennessee 37830

Abstract

The theory of unfavorable curvature-driven instabilities is developed for a plasma interacting with a hot electron ring whose drift frequencies are larger than the growth rates predicted from conventional magnetohydrodynamic theory. A z-pinch model is used to emphasize the radial structure of the problem. Stability criteria are obtained for the five possible modes of instability: the conventional hot electron interchange, a high-frequency hot electron interchange (at frequencies larger than the ion cyclotron frequency), a compressional instability, a background pressure-driven interchange, and an interacting pressure-driven interchange.

I. INTRODUCTION

Experimental evidence[1,2] has shown conclusively that plasmas containing hot electrons can be stable in magnetic well configurations that would be predicted to be highly unstable in conventional magnetohydrodynamic (MHD) fluid theory. However, conventional MHD theory can break down because the hot electron drift frequency is larger than the conventional MHD ordering. Specifically, the hot electron curvature drift frequency can be larger than the predicted MHD growth rates and even larger than the ion cyclotron frequency. These effects need to be included when considering an appropriate theory for hot electron instability, and thus predictions different from those of MHD theory can be expected.

Several authors have included additional physics in describing the stability of hot electron plasmas. Krall[3] considered the effect of cold plasma on the hot electron interchange instability and showed that, with a sufficiently large amount of cold plasma, the mode is stabilized. Berk[4] extended Krall's model to describe stability when the hot electron drift frequency exceeds the ion cyclotron frequency. Dominguez and Berk[5] treated the electromagnetic aspects of the problem in a self-consistent fashion and verified the results of Krall[3] and of Berk.[4] They also showed that a hot electron interchange mode, distinct from the conventional MHD mode, can exist at frequencies above the ion cyclotron frequency.

Given a mechanism for stabilizing the hot electron interchange, it had been shown[6] that the diamagnetic well produced by the hot electrons could stabilize the background plasma as long as its beta, β_c, was less than half the hot electron beta, β_h, where the beta value of a plasma is defined as $\beta = 2P/B^2$, with P its pressure and B the magnetic field strength. However, Van Dam and Lee[7] and also Nelson[8] showed that the background plasma is stabilized with respect to a background pressure-driven interchange instability only if a more stringent condition is met, viz., $\beta_c < 2\Delta/R$, where Δ is the annulus thickness and R the unfavorable radius of curvature.

However, Van Dam et al.[9] then developed a generalized energy principle (similar to one developed by Antonsen et al.[10]) to account for the high hot electron drift frequency, which predicted a stability picture more pessimistic than even the conventional Kruskal-Oberman[11] energy principle. Hence the theoretical explanation of stability in the Elmo Bumpy Torus (EBT) appeared elusive. However, it can be shown[10] that this new energy principle only yields a sufficient condition for stability, (if particle resonances are ignored) so that a prediction for instability requires a more complicated modal analysis. Recent independent calculations by El Nadi[12,13] and our group[14] have established that a new compressional mode is present if the background density is too high. The unstable compressional mode is seen to be responsible for the pessimistic energy principle prediction. However, with the modal analysis, stability is found to be possible at moderate background plasma density values. This compressional mode has also been applied to tandem mirrors by Rosenbluth.[15]

All the works we have alluded to (with the exception of Ref.13) use models that describe stability at one radial point. In this paper, we develop a self-consistent hot electron plasma theory that attempts to treat radial aspects of the problem more realistically. In addition, we have analyzed some aspects of the axially-dependent problem, which are discussed elsewhere.[16]

To treat the radial problem, we model the plasma as a z-pinch with a hot electron annulus present. The z-pinch model has the virtue that magnetic field line curvature is present in a natural way, rather than by being introduced through an ad hoc gravity. In this model, the system has two ignorable coordinates, and a second-order radial differential equation can be derived for the response of the system. The mode structure across the annulus can then be determined. We find that there is a set of short-wavelength WKB modes that are similar to those of local theory, although the geometry places restrictions on the perpendicular wavenumbers that strongly affect growth rates and stability limits. In addition, one finds layer modes, with long radial wavelengths over the annulus region.

In Section II we derive the basic differential equation for the z-pinch model. In Section III we give an overview of the modes contained in the differential equation. In Section IV we analyze the mode structure of our equation. A summary of our results is presented in Section V, and any reader not interested in the detailed analysis is referred to this final section.

II. DERIVATION OF RADIAL EIGENMODE EQUATION

We will derive the radial eigenmode equation for a hot electron plasma in a z-pinch model as shown in Fig. 1. The hot electrons are contained in an annular cylindrical shell, and the magnetic field is in the $-\hat{\theta}$ direction. Note that the θ- and z-directions of the z-pinch cylindrical geometry then represent the (anti)toroidal and poloidal directions, respectively, of a bumpy torus. The symmetry in the θ and z directions enables us to obtain an exact radial differential equation for the system.

In equilibrium the hot electrons create a diamagnetic well that can be used to stabilize the background plasma if the hot electrons are passive to perturbations. However, as the hot electrons are not passive, several types of oscillations can arise that may cause instability. The frequencies of interest can be comparable to the ion cyclotron frequency, but much less than the electron cyclotron frequency. This simplifies the analysis, since the electron response can be treated entirely in the low frequency limit. It is, however, necessary to keep the high frequency response of the ions. The simplest method is to take the ion response in the cold plasma limit. However, because finite background pressure is important in the theory, we will treat the background electrons with finite pressure. Our analysis will be in the zero Larmor radius limit so that perturbations conserve the lowest-order magnetic moment.

We will formulate the equation in terms of fluid equations, with the pressure response being determined from the second moment of the Vlasov equation. For the inertial response, we need only account for ion dynamics. Since the ions are taken in the cold plasma limit, we obtain a relatively simple finite frequency expression for their response.

We shall assume charge neutrality and also $\underset{\sim}{E} \cdot \hat{\underset{\sim}{b}} = 0$, where $\underset{\sim}{E}$ is the electric field and $\hat{\underset{\sim}{b}}$ is the unit vector in the direction of the equilibrium magnetic field. The fluid equation for the system is

$$\frac{\partial}{\partial t}\rho\underset{\sim}{V} = -\underset{\sim}{\nabla} \cdot \underset{\sim}{\underset{\sim}{P}} + \left(\underset{\sim}{\nabla} \times \underset{\sim}{B}\right) \times \underset{\sim}{B} \quad , \tag{1}$$

where the pressure tensor $\underset{\sim}{\underset{\sim}{P}}$ is defined as

$$\underset{\sim}{\underset{\sim}{P}} = \sum_j \int F_j \underset{\sim}{v}\underset{\sim}{p} d^3p \quad , \tag{2}$$

ρ is the mass density, $\underset{\sim}{V}$ is the fluid velocity, F_j is the distribution function for the j^{th} species, and electrons are treated relativistically so that the momentum $\underset{\sim}{p}$ is related to the particle velocity $\underset{\sim}{v}$ by $\underset{\sim}{p} = m_j\gamma\underset{\sim}{v}$ with $\gamma = \left(1 - v^2/c^2\right)^{-1/2}$. In the zero Larmor radius limit, the pressure tensor has the diagonal form

$$\underset{\sim}{\underset{\sim}{P}} = \sum_j \int\int \frac{dH d\mu B}{|p_\parallel|} F_j(r,H,\mu)\left[\mu B\left(\underset{\sim}{\underset{\sim}{I}} - \hat{\underset{\sim}{b}}\hat{\underset{\sim}{b}}\right) + p_\parallel^2 \hat{\underset{\sim}{b}}\hat{\underset{\sim}{b}}\right]$$

$$\equiv P_\perp\left(\underset{\sim}{\underset{\sim}{I}} - \hat{\underset{\sim}{b}}\hat{\underset{\sim}{b}}\right) + P_\parallel \hat{\underset{\sim}{b}}\hat{\underset{\sim}{b}} \quad , \tag{3}$$

where $c^2 p_\parallel^2 = H^2 - 2\mu Bc^2 - m_j^2 c^4$, H is the relativistic energy, and $\mu = p_\perp^2/2B$ is the magnetic moment. Equation (1) can then be written as

$$\frac{\partial}{\partial t}\rho\underset{\sim}{V} = -\underset{\sim}{\nabla}\left(P_\perp + \frac{B^2}{2}\right) + \underset{\sim}{\nabla}\cdot\left\{\underset{\sim}{BB}\left[1 - \frac{(P_\parallel - P_\perp)}{B^2}\right]\right\} \quad . \qquad (4)$$

A convenient reduction of this equation is to take the scalar product of $\underset{\sim}{B}$ with the curl of Eq. (4). After some algebraic manipulations (see Appendix A), one obtains the equation

$$\underset{\sim}{\nabla}\cdot\left[\underset{\sim}{B}\times\rho\dot{\underset{\sim}{V}}\right] + B^2\left(\underset{\sim}{B}\cdot\underset{\sim}{\nabla}\right)\left(\frac{\sigma\underset{\sim}{J}\cdot\underset{\sim}{B}}{B^2}\right) - \left(\underset{\sim}{B}\times\underset{\sim}{\kappa}\right)\cdot\underset{\sim}{\nabla}\left(\frac{B^2}{2} - P_\parallel\right)$$

$$+ \rho\dot{\underset{\sim}{V}}\cdot\left(\hat{\underset{\sim}{b}}\times\underset{\sim}{\nabla}B\right) = 0 \quad . \qquad (5)$$

where $\underset{\sim}{\kappa} = (\hat{\underset{\sim}{b}}\cdot\underset{\sim}{\nabla})\hat{\underset{\sim}{b}}$ and $\sigma = 1 - (P_\parallel - P_\perp)/B^2$. Note that in the z-pinch model, Eq. (5) is trivially satisfied in equilibrium.

The equation for $F_j(\underset{\sim}{r},H,\mu)$ satisfies the drift kinetic Vlasov equation, which in the low frequency, zero Larmor radius limit takes the form

$$\frac{\partial F_j}{\partial t} + v_\parallel\hat{\underset{\sim}{b}}\cdot\underset{\sim}{\nabla}F_j + \underset{\sim}{v}_d\cdot\frac{\partial F_j}{\partial r} + \dot{H}\frac{\partial F_j}{\partial H} = 0 \quad , \qquad (6)$$

where

$$v_{\parallel} = \frac{p_{\parallel}}{\gamma m_j} = \pm \frac{1}{\gamma c^2 m_j} \left[H^2 - 2\mu B c^2 - m_j^2 c^4 \right]^{1/2} \tag{7}$$

$$\underset{\sim}{v}_d = \frac{\mu \hat{\underset{\sim}{b}} \times \underset{\sim}{\nabla} B}{q_j m_j B \gamma} + \frac{p_{\parallel}^2}{q_j m_j B \gamma} \left[\hat{\underset{\sim}{b}} \times \left(\hat{\underset{\sim}{b}} \cdot \underset{\sim}{\nabla} \right) \hat{\underset{\sim}{b}} \right] + \frac{\underset{\sim}{E} \times \hat{\underset{\sim}{b}}}{B} \tag{8}$$

$$\dot{H} = q_j E_{\parallel} v_{\parallel} + q_j \underset{\sim}{E}_{\perp} \cdot \underset{\sim}{v}_d + \frac{\mu}{\gamma m_j} \frac{\partial B}{\partial t} . \tag{9}$$

For the z-pinch, the equilibrium drifts are in the $\hat{\underset{\sim}{z}}$ direction, and hence the equilibrium distribution can be taken as a function $F_0(r,H,\mu)$. The radial pressure balance condition for Eq. (1) then yields

$$\frac{d}{dr}\left(\frac{B^2}{2} + P_{\perp} \right) = \frac{-B^2}{r} \left[1 - \frac{\left(P_{\parallel} - P_{\perp} \right)}{B^2} \right] , \tag{10}$$

where $-1/r$ is the field line curvature and $P_{\parallel,\perp}$ the equilibrium pressure components.

We now consider the linear response of the perturbed fluid equations to a "displacement" $\underset{\sim}{\xi}$, defined in terms of the perturbed electric field $\underset{\sim}{E}_1$ as

$$\underset{\sim}{\xi} \equiv i \frac{\underset{\sim}{E}_1(r) \times \hat{\underset{\sim}{b}}}{\omega B} \exp\left[-i\omega t + ikz \right] \tag{11}$$

where we restrict ourselves to flute-like perturbations. From the induction equation, the perturbed magnitude of $\underset{\sim}{B}$ is

$$B_1 = -\hat{\underset{\sim}{\theta}} \cdot \underset{\sim}{\nabla} \times (\underset{\sim}{\xi} \times \underset{\sim}{B}) = -\left[\frac{d}{dr}(\xi_r B) + ik\xi_z B\right] \tag{12}$$

where $B \equiv |\underset{\sim}{B}|$.

The linearly perturbed z-component of Eq. (4) yields

$$\begin{aligned} -i\omega\rho V_{1z} &= -ik(BB_1 + P_{\perp 1}) \\ &= k\left[-kB^2\xi_z + iB\frac{d}{dr}(B\xi_r) - iP_{\perp 1}\right] . \end{aligned} \tag{13}$$

The perturbed velocity $\underset{\sim}{V}_1$ is obtained using the response of a cold ion fluid, which is simply the linear response of a single particle. Hence we have

$$-i\omega\underset{\sim}{V}_1 - (\underset{\sim}{V}_1 \times \hat{\underset{\sim}{b}})\,\omega_{ci} = i\omega\omega_{ci}\underset{\sim}{\xi}\times\hat{\underset{\sim}{b}} , \tag{14}$$

$$-i\omega\underset{\sim}{V}_1\times\hat{\underset{\sim}{b}} + \omega_{ci}\underset{\sim}{V}_1 = -i\omega\omega_{ci}\underset{\sim}{\xi} , \tag{15}$$

where $\omega_{ci} = q_i B/m_i$ is the ion cyclotron frequency. Solving for $-i\omega\rho\underset{\sim}{V}_1$ yields

$$-i\omega\rho\underset{\sim}{V}_1 = -\lambda\rho\left[\underset{\sim}{\xi} + \frac{i\omega}{\omega_{ci}}(\underset{\sim}{\xi}\times\hat{\underset{\sim}{b}})\right] , \tag{16}$$

where $\lambda = \omega_{ci}^2\omega^2/(\omega_{ci}^2 - \omega^2)$. Hence, Eq. (13) may be written as

$$-ik\xi_r B\frac{dB}{dr} + ikP_{\perp 1} = -k\left(kB^2\xi_z - iB^2\frac{d\xi_r}{dr}\right) + \lambda\rho\left(\dot{\xi}_z - i\frac{\omega}{\omega_{ci}}\xi_r\right). \tag{17}$$

We now obtain the perturbed version of Eq. (5), which has the form

$$\omega k\rho BV_{1r} + i\omega\frac{B}{r}\frac{d}{dr}(\rho rV_{1z}) + i\frac{kB}{r}(BB_1 - P_{\parallel 1}) = 0, \tag{18}$$

or

$$\omega k\rho BV_{1r} + i\omega\frac{B}{r}\frac{d}{dr}(\rho rV_{1z}) + k\frac{B^3}{r}\left[k\xi_z - \frac{i}{B}\frac{d}{dr}(\xi_r B) - \frac{iP_{\parallel 1}}{B^2}\right] = 0. \tag{19}$$

The perturbed pressure components $P_{\parallel 1}$ and $P_{\perp 1}$ are given by

$$\begin{pmatrix} P_{\parallel 1} \\ P_{\perp 1} \end{pmatrix} = -\hat{\underset{\sim}{\theta}}\cdot\underset{\sim}{B}_1\begin{pmatrix} \partial P_\parallel/\partial B \\ \partial P_\perp/\partial B \end{pmatrix} + \sum_j\int\frac{dHd\mu B}{|p_\parallel|}f_j\begin{pmatrix} \mu B \\ p_\parallel^2 \end{pmatrix}, \tag{20}$$

where the perturbed distribution function f_j is determined by the linearized form of the Vlasov equation given by Eq. (6). For $\partial P_\parallel/\partial B$ and $\partial P_\perp/\partial B$, we may use the identities

$$\frac{\partial P_\perp}{\partial B} = -B \sum_j \int \frac{dH d\mu}{|p_\parallel|} \mu^2 \frac{\partial F_j}{\partial \mu} , \tag{21}$$

$$\frac{\partial P_\parallel}{\partial B} = -\sum_j \int dH d\mu \mu |p_\parallel| \frac{\partial F_j}{\partial \mu} . \tag{22}$$

The linearized form of the Vlasov equation (for no equilibrium electric field) is

$$\frac{Df_j}{Dt} = -\underset{\sim}{v}_{d1} \cdot \hat{\underset{\sim}{r}} \frac{\partial F_j}{\partial r} - \left(-i\omega \frac{\mu B_1}{\gamma m_j} + q_j \underset{\sim}{E}_{1\perp} \cdot \underset{\sim}{v}_d \right) \frac{\partial F_j}{\partial H} , \tag{23}$$

where

$$\frac{D}{Dt} = -i(\omega - \omega_{db} - \omega_{cv}) \equiv -i\Omega , \tag{24}$$

$$\omega_{db} = \frac{k\mu}{q_j m_j B \gamma} \frac{dB}{dr} , \tag{25}$$

$$\omega_{cv} = -\frac{k p_\parallel^2}{q_j m_j B \gamma r} , \tag{26}$$

and

$$\underset{\sim}{v}_{d1} \cdot \hat{\underset{\sim}{r}} = -ik \frac{\mu B_1}{q_j \gamma m_j B} - i\omega \xi_r . \tag{27}$$

Equation (23) is then solved for f_j to yield

$$f_j = -\xi_r \frac{\partial F}{\partial r} - \frac{\left(\frac{k}{q_j B}\frac{\partial F}{\partial r} + \omega \frac{\partial F}{\partial H}\right)}{\Omega m_j \gamma}\left(\mu\tilde{B} - \frac{p_\parallel^2}{r}\xi_r\right) , \qquad (28)$$

where $\tilde{B}$ is the perturbed magnetic field strength in the Lagrangian sense:

$$\tilde{B} = B_1 + \xi_r \frac{\partial B}{\partial r} = -B\left(\frac{\partial \xi_r}{\partial r} + ik\xi_z\right) . \qquad (29)$$

Solving for $P_{\perp 1}$ and $P_{\parallel 1}$ then yields

$$P_{\perp 1} = -\left[\frac{dP_\perp}{dr} + \frac{\left(G_2 - \frac{\partial P_\parallel}{B\partial B}\right)}{r} B^2\right]\xi_r + \tilde{B}BG_1$$

$$= \left[B\frac{dB}{dr} + \frac{(1 - G_2)}{r} B^2\right]\xi_r + \tilde{B}BG_1 \qquad (30)$$

$$P_{\parallel 1} = -\xi_r\left(\frac{dP_\parallel}{dr} + \frac{B^2 G_3}{r}\right) + BG_2\tilde{B} \qquad (31)$$

where we have used the equilbrium conditions

$$\frac{dP_\perp}{dr} = -B\frac{dB}{dr} - \frac{B^2}{r}\sigma \qquad (32)$$

and

$$\frac{\partial P_{\parallel}}{B\partial B} = 1 - \sigma \quad , \tag{33}$$

and we have defined

$$G_1 = \frac{\partial P_{\perp}}{B\partial B} - B \sum_j \int \frac{dH d\mu \mu^2}{|p_{\parallel}|} \frac{\left(\frac{k}{q_j B} \frac{\partial F}{\partial r} + \omega \frac{\partial F}{\partial H} \right)}{\Omega m_j \gamma}, \tag{34}$$

$$G_2 = \frac{\partial P_{\parallel}}{B\partial B} - \sum_j \int dH d\mu \mu |p_{\parallel}| \frac{\left(\frac{k}{q_j B} \frac{\partial F}{\partial r} + \omega \frac{\partial F}{\partial H} \right)}{\Omega m_j \gamma}. \tag{35}$$

$$G_3 = -\frac{1}{B} \sum_j \int dH d\mu |p_{\parallel}|^3 \frac{\left(\frac{k}{q_j B} \frac{\partial F}{\partial r} + \omega \frac{\partial F}{\partial H} \right)}{\Omega m_j \gamma} \tag{36}$$

In our z-pinch model, $p_{\parallel}$ is a constant of motion. Thus, if F is written as $F(p_{\parallel},\mu,r)$, and if we use the identities of Eqs. (21) and (22) for $\partial P_{\perp}/\partial B$ and $\partial P_{\parallel}/\partial B$, Eqs. (34) through (36) can be rewritten as

$$G_1 = -B \sum_j \int \frac{dp_{\parallel} d\mu \mu^2}{\gamma m_j} \left[\frac{1}{B} \frac{\partial F}{\partial \mu} + \frac{\left(\frac{k}{m_j q_j B} \frac{\partial F}{\partial r} + \frac{\gamma \omega_{cv}}{p_{\parallel}} \frac{\partial F}{\partial p_{\parallel}} \right)}{\gamma \Omega} \right], \tag{34'}$$

$$G_2 = -\sum_j \int \frac{dp_{\parallel} d\mu \mu}{\gamma m_j} p_{\parallel}^2 \left[\frac{1}{B} \frac{\partial F}{\partial \mu} + \frac{\left(\frac{k}{m_j q_j B} \frac{\partial F}{\partial r} + \frac{\gamma \omega_{cv}}{p_{\parallel}} \frac{\partial F}{\partial p_{\parallel}} \right)}{\gamma \Omega} \right], \tag{35'}$$

$$G_3 = -\frac{1}{B}\sum_j \int \frac{dp_\parallel d\mu p_\parallel^4}{\gamma m_j}\left[\frac{1}{p_\parallel}\frac{\partial F}{\partial p_\parallel} + \frac{\left(\frac{k}{m_j q_j B}\frac{\partial F}{\partial r} + \frac{\gamma\omega_{cv}}{p_\parallel}\frac{\partial F}{\partial p_\parallel}\right)}{\gamma\Omega}\right] . \quad (36')$$

Combining Eqs. (17) and (30) leads to the relation

$$\left[ik\frac{(1-G_2)}{r}B^2 + \frac{i\omega}{\omega_{ci}}\lambda\rho - ikB^2(1+G_1)\frac{d}{dr}\right]\xi_r \ , \quad (37)$$

whereas combining Eqs. (16), (19), and (31) leads to

$$\left[-k^2B^3\frac{(1-G_2)}{r} - \lambda k\rho B\frac{\omega}{\omega_{ci}}\right]\xi_z - \frac{B}{r}\frac{d}{dr}(r\lambda\rho\xi_z)$$

$$= \left[i\frac{kB}{r}\frac{d}{dr}(P_\perp + P_\parallel) + i\frac{kB^3}{r^2}(\sigma + G_3) - iB\lambda k\rho\right]\xi_r$$

$$-iB^3\frac{(1-G_2)}{r}k\frac{d\xi_r}{dr} - i\frac{B}{r}\frac{d}{dr}\left(\lambda\rho\frac{r\omega}{\omega_{ci}}\xi_r\right) . \quad (38)$$

Combining these equations, (37) and (38), we finally obtain the governing differential equation:

$$\left\{ \frac{\lambda k^2 r(1 + G_1)\rho}{Q} - \frac{d}{dr}\left[\frac{\lambda(1 + G_1)\rho r}{Q} \right] \frac{d}{dr} \right\} \xi$$

$$+ \xi \left(\frac{-\omega^2}{V_A^2} \frac{r\lambda\rho}{Q} - k^2 B^2 \left\{ \frac{1}{B^2} \frac{d}{dr} \left(P_\perp + P_\parallel \right) \right.\right.$$

$$\left. + \frac{1}{r}\left[\sigma - \frac{(1 - G_2)^2}{Q} \right] + \frac{G_3}{r} \right\} + \frac{2\omega\lambda(1 - G_2)k\rho}{\omega_{ci} Q}$$

$$\left. + \frac{d}{dr}\left[\frac{\rho\lambda(1 - G_2) + \rho \frac{\lambda\omega r k}{\omega_{ci}} (1 + G_1)}{Q} \right] \right) = 0, \qquad (39)$$

where $\xi = \xi_r$, $V_A^2 = B^2/\rho$ is the Alfvén speed, and $Q = 1 + G_1 - \lambda/k^2 V_A^2$.

III. GENERAL MODE STRUCTURE

Let us briefly discuss the general structure of Eq. (39) before performing a detailed analysis. We will show how the usual MHD modes arise and how they are altered in a hot electron plasma.

In conventional MHD theory, one assumes small drifts, that is, $\omega_{dj} << \omega$ and

$$\frac{k}{q_j B}\frac{\partial F_j}{\partial r} << \omega \frac{\partial F_j}{\partial H} ,$$

and also $\gamma \simeq 1$ (nonrelativistic). In this limit we find

$$G_1 = \frac{1}{B}\frac{\partial P_\perp}{\partial B} - \sum_j \frac{B}{m_j}\int \frac{dH d\mu \mu^2}{|p_\parallel|}\frac{\partial F_j}{\gamma \partial H} \xrightarrow{\gamma=1} \frac{2P_\perp}{B^2} \equiv \beta_\perp , \tag{40}$$

$$G_2 = \frac{1}{B}\frac{\partial P_\parallel}{\partial B} - \sum_j \frac{1}{m_j}\int dH d\mu \mu |p_\parallel| \frac{\partial F_j}{\gamma \partial H} \xrightarrow{\gamma=1} \frac{P_\parallel}{B^2} \equiv \frac{\beta_\parallel}{2} , \tag{41}$$

$$G_3 = -\sum_j \frac{1}{Bm_j}\int dH d\mu |p_\parallel|^3 \frac{\partial F_j}{\gamma \partial H} \xrightarrow{\gamma=1} \frac{3}{2}\beta_\parallel . \tag{42}$$

If we consider $\omega/\omega_{ci} << 1$ and set $(1 + G_1)/Q = 1$, Eq. (39) then becomes

$$\underset{(1)}{\left[k^2 - \frac{1}{\rho r}\frac{d}{dr} r\rho \frac{d}{dr}\right]}\xi - \left(\underset{(2)}{\frac{\omega^2}{V_A^2(1 + \beta_\perp)}} + \frac{k^2 V_A^2}{\omega^2 r}\left\{ \underset{(3)}{\frac{1}{B^2}\frac{d}{dr}(P_\parallel + P_\perp) + \frac{1}{r}\left[\sigma + \frac{3}{2}\beta_\parallel - \frac{\left(1 - \frac{\beta_\parallel}{2}\right)^2}{(1 + \beta_\perp)}\right]}\right\}\right)\xi = 0 \quad . \tag{43}$$

Equation (43) recovers modes associated with double adiabatic theory. In the limit of large k, we may balance terms (1) and (3) to find

$$\omega^2 = \frac{V_A^2}{r}\left\{\frac{1}{B^2}\frac{d}{dr}(P_\parallel + P_\perp) + \frac{1}{r}\left[\sigma + \frac{3}{2}\beta_\parallel - \frac{\left(1 - \frac{\beta_\parallel}{2}\right)^2}{1 + \beta_\perp}\right]\right\} \quad , \tag{44}$$

which is the interchange mode for double adiabatic theory including terms from compression. This leads to the usual instability that is driven by the product of pressure gradient and curvature. In addition, there is a stable oscillation obtained by balancing terms (1) and (2) in Eq. (43), which is the compressional Alfvén wave:

$$\omega^2 = k_\perp^2 V_A^2 (1 + \beta_\perp) \quad , \tag{45}$$

where $k_\perp^2 \approx k^2 - d^2/dr^2$.

Now for a hot electron plasma, the above results are altered considerably because the natural ordering for hot electrons, when $|\nabla B/B| \equiv |\Delta_b^{-1}| >> 1/r$, is (with $q_e = -|e|$)

$$\frac{k}{q_e B} \frac{\partial F}{\partial r} >> \omega \frac{\partial F}{\partial H} ,$$

$$\omega_{db} >> \omega, \omega_{cv} .$$

The condition $\Delta_b << r$ means that the high pressure of the hot electrons is mostly supported by a deep diamagnetic well in equilibrium force balance.

If we now use the expansion

$$\frac{1}{\Omega} \simeq -\frac{1}{\omega_{db}} - \frac{(\omega - \omega_{cv})}{\omega_{db}^2} + O\left[\left(\frac{\Delta_b}{r}\right)^2\right] , \tag{46}$$

we find that Eqs. (34) - (36) may be approximated, for $\Delta_b << r$, as

$$1 + G_1 = -\left(\frac{r}{B}\frac{dB}{dr}\right)^{-1}\left(1 - \frac{dP_{\parallel h}/dr}{BdB/dr}\right) - \frac{\omega}{\bar{\omega}_{db}} - \left(\frac{dP_{\perp c}/dr}{BdB/dr} - \beta_{\perp c}\right), \quad (47)$$

$$G_2 = \frac{\beta_{\parallel c}}{2} + \frac{dP_{\parallel h}/dr}{BdB/dr}, \quad (48)$$

$$G_3 = \frac{3}{2}\beta_{\parallel c}, \quad (49)$$

where "c" refers to the background plasma and "h" to the hot electron plasma and where

$$\bar{\omega}_{db} = \frac{-k\left(\frac{dB}{dr}\right)^2}{q_e B^2 \frac{d}{dr}\left(\frac{n_h}{B}\right)} \approx \frac{km_e\langle V_h^2\rangle}{q_e B^2}\frac{dB}{dr} \quad (50)$$

with

$$\langle V_h^2\rangle \equiv \frac{\frac{1}{B^2 m_e}\frac{dP_{\perp h}}{dr}}{\frac{d}{dr}\left(\frac{n_h}{B}\right)}. \quad (51)$$

[It can be shown that the form of Eqs. (47) - (49) is correct, in the $\Delta_b/r << 1$ limit, even for hot electrons that are relativistic.] The result is that, in the hot electron limit, the differential equation, (39), is found to be

(1)

$$\left[\frac{-\lambda\alpha\Delta_b\left(1-\delta_c'-\frac{\omega}{\bar{\omega}_{cv}}\right)}{Q}\rho k^2+\frac{d}{dr}\frac{\rho\lambda\alpha\Delta_b\left(1-\delta_c'-\frac{\omega}{\bar{\omega}_{cv}}\right)}{Q}\frac{d}{dr}\right]_\xi$$

(2) (3)

$$+\xi\left\{-\frac{\omega^2}{V_A^2}\frac{r\lambda\rho}{Q}-k^2\left(\frac{dP_{\parallel c}}{dr}+\frac{3P_{\parallel c}}{r}\right)\right.$$

$$-\frac{rk^2B^2}{\Delta_b}\frac{\left[\frac{d}{dr}\left(\frac{P_{\perp c}}{B^2}\right)+\frac{2P_{\parallel c}}{rB^2}\left(1-\frac{1}{2\alpha}\frac{P_{\parallel c}}{B^2}\right)+\frac{\lambda}{k^2V_A^2\Delta_b}-\frac{\alpha\omega}{r\bar{\omega}_{cv}}\right]}{\left(1-\delta_c'-\frac{\omega}{\bar{\omega}_{cv}}+\frac{\lambda r}{\alpha\Delta_b k^2V_A^2}\right)}$$

(4) (5)

$$\left.+\frac{\omega\rho k(2\alpha-\beta_{\parallel c})\lambda}{\omega_{ci}Q}+\frac{d}{dr}\left[\frac{\lambda\rho(\alpha-\beta_{\parallel c}/2)-\frac{\rho\lambda\omega\Delta_b}{\omega_{ci}}\alpha k\left(1-\delta-\frac{\omega}{\bar{\omega}_{cv}}\right)}{Q}\right]\right\}$$

$$=0\ . \tag{52}$$

where

$$\alpha=1-\frac{dP_{\parallel h}/dr}{B(dB/dr)} \tag{53}$$

$$\delta_c'=-\frac{r}{\alpha}\frac{d}{dr}\left(\frac{P_{\perp c}}{B^2}\right) \tag{54}$$

and

$$\bar{\omega}_{cv} = \frac{-\bar{\omega}_{db}\alpha\Delta_b}{r} \quad , \tag{55}$$

with the quantity Q that was defined following Eq. (39) as being given by

$$Q = \frac{-\alpha\Delta_b}{r}\left(1 - \delta_c' - \frac{\omega}{\bar{\omega}_{cv}}\right) - \frac{\lambda}{k^2 V_A^2} \quad . \tag{56}$$

Equation (52) has an entirely different structure than Eq. (43). Now, if we balance terms (1) and (3) of Eq. (52) in the limit

$$1 \gg \left[\frac{\omega}{\bar{\omega}_{cv}}, \frac{\omega}{k_\perp V_A}\left(\frac{r}{\Delta_b}\right)^{1/2}, \frac{\omega}{\omega_{ci}}, \beta_{\perp h}\right] \quad ,$$

we obtain

$$\omega^2 \simeq \left(\frac{k^2}{k_\perp^2}\right) V_A^2 \left\{ \frac{1}{rB^2}\frac{dP_{\parallel c}}{dr} - \frac{\frac{1}{B}\frac{dB}{dr}\frac{d}{dr}\left(\frac{P_{\perp c}}{B^2}\right)}{\left[1 + \frac{r}{\alpha}\frac{d}{dr}\left(\frac{P_{\perp c}}{B^2}\right)\right]} \right\} \quad . \tag{57}$$

This is the dispersion relation found by Van Dam and Lee[7] and by Nelson[8] for the low-frequency interacting interchange mode. At low β_c such that $1 \gg -(r/\alpha)(d/dr)(P_{\perp c}/B^2)$, only the cold plasma pressure drives

the interchange instability, and stability is achieved when the magnetic gradient of the diamagnetic well overcomes the curvature

$$\frac{dB}{Bdr}\left|\frac{dP_{\perp c}}{dr}\right| > \frac{1}{r}\left|\frac{dP_{\parallel c}}{dr}\right| \quad . \tag{58}$$

However, the sign of the diamagnetic term changes when

$$-\frac{r}{\alpha}\frac{d}{dr}\left(\frac{P_{\perp c}}{B^2}\right) \geq 1 \quad , \tag{59}$$

in which case the interchange mode is destabilizing. Well above this threshold, when

$$-\frac{r}{\alpha}\frac{d}{dr}\left(\frac{P_{\perp c}}{B^2}\right) >> 1 \quad ,$$

Eq. (57) becomes the usual expression for the interchange mode in the weak curvature limit,

$$\omega^2 \simeq \frac{k^2 V_A^2}{k_\perp^2}\left[\frac{1}{rB^2}\frac{d}{dr}\left(P_\parallel + P_\perp\right)\right], \tag{60}$$

where now the total pressure enters.

Balancing terms (1) and (2) of Eq. (52) in the limit $\omega/\bar{\omega}_{cv} << 1$ gives rise to a compressional magnetic instability, rather than the compressional Alfvén wave of the usual MHD ordering. For this instability, the local dispersion relation is seen to be

$$\omega^2 = -\alpha k_\perp^2 V_A^2 (1 - \delta_c') \frac{\Delta_b}{r} \quad . \tag{61}$$

We see that this mode is unstable when $\delta_c' < 1$ and $\Delta_b/r > 0$, roughly the same as the conditions to stabilize the interchange mode. Thus, if we assume $\omega/\bar{\omega}_{cv} << 1$, when the interchange mode is stable the compressional mode is not. The recent analysis of Van Dam et al.[9] showing that the low-frequency energy principle is more pessimistic than conventional guiding center MHD theory is due to the presence of this mode. This mode is closely related to the magnetic trapped particle mode reported by Rosenbluth[14] and has been independently found by El-Nadi.[12]

It should be also noted that the conventional hot electron interchange, with $\omega << \omega_{ci}$, can be obtained by balancing terms (1) and (3) when $\omega/\bar{\omega}_{cv} >> 1$. It is this mode that is stabilized by cold background, as reported by Krall.[3]

The high-frequency hot electron interchange mode[5] is obtained by observing that if $\omega_{ci} << \omega << \bar{\omega}_{cv}$ and $n_h = n_c$ (with n_c the background ion density), then the last expression in term (3) of Eq. (52) cancels most of term (5), with the remainder of term (5) being balanced with term (1) to give $\omega^2 = -\omega_{ci}\bar{\omega}_{cv}k_\perp^2\Delta/k$, with $\Delta = -\rho^{-1}(d\rho/dr)$.

IV. DETAILED ANALYSIS

We now analyze the modes of Eq. (39) in more detail to obtain stability criteria. If $\Delta_b/r << 1$, we saw that the kinetic terms can be expressed in terms of density and pressure. However, in actual experimental operation, the value of Δ_b/r is not much smaller than unity (where we associate r with the experimental magnetic field radius of curvature), so that the forms in Eq. (49) can be quantitatively inaccurate. Alternatively, we can choose a simple hot electron distribution function of the form

$$F_h = m_e \delta(p_\parallel)\delta(\mu - \mu_0)\, \gamma_0 \frac{P_{\perp h}(r)}{[\, B^2(r)\mu_0 \,]}, \tag{62}$$

where $P_{\perp h}(r)$ is the perpendicular hot electron pressure, $\gamma_o^2 = 1 + 2\mu_o B(r)/m^2c^2$, and the parallel hot electron pressure is zero. This distribution allows us to treat Δ_b/r arbitrarily and to have a tractible algebraic form. For this distribution, Eqs. (34′) - (36′) become

$$1 + G_1 =$$

$$\frac{\omega\left(1 + \beta_\perp - \beta_{\perp h}\dfrac{\mu_0 B}{2\gamma_0^2 m_e^2 c^2}\right) - \omega_{cv\perp}\left[1 + \dfrac{(\beta_{\perp c} - \beta_{\parallel c})}{2} + r\dfrac{d}{dr}\left(\dfrac{P_{\perp c}}{B^2}\right)\right]}{\omega - \omega_{db}}, \tag{63}$$

$$G_2 = \frac{\beta_{\parallel} c}{2} , \tag{64}$$

and

$$G_3 = \frac{3\beta_{\parallel} c}{2} . \tag{65}$$

Here we have assumed that ω is greater than the background plasma drift frequencies and used the nonrelativistic fluid-type response of Eqs. (40) - (42) for the background plasma species. Also, we have defined effective curvature and gradient-B drift frequencies for the hot electrons (both evaluated at the transverse energy) as

$$\omega_{cv\perp} = -\frac{k\mu_0}{q_e m_e \gamma_0 r} , \tag{66}$$

$$\omega_b = \frac{k\mu_0}{q_e m_e \gamma_0 B} \frac{dB}{dr} . \tag{67}$$

We have been able to show that using these forms for G_1, G_2, and G_3, rather than the forms in Eqs. (47) - (49), leads to qualitatively the same stability criteria as when $\Delta_b/r << 1$.

The radial eigenmode equation, (39), admits two types of modes: "layer modes" with $\xi(r)$ nearly constant over the hot electron layer and decaying outside the layer; and WKB-type modes with $k_r\Delta \simeq (n + \nu)\pi$, where k_r is the radial wavelength, Δ the length over which the background pressure falls off in the layer, and $\nu \sim 1$.

A. Layer Modes

For the layer modes, we integrate Eq. (39) across the electron annulus, with the assumption that $\xi(r)$ is nearly constant, to obtain

$$\int_{r^-}^{r^+} dr \left\{ \underbrace{\lambda\rho r k^2}_{(1)} + \underbrace{\frac{\omega^2\lambda^2\rho r}{\omega_{ci}^2 V_A^2 Q}}_{(2)} - \underbrace{\frac{k^2 B^2}{r}}_{(3)} \underbrace{\left[G_3 - \frac{(1 - G_2)^2}{Q} \right]}_{(4)} + \underbrace{\frac{2\omega\lambda\rho}{\omega_{ci}} \frac{(1 - G_2)}{Q} k}_{(5)} \right\}$$

$$= \left[\underbrace{\frac{\lambda\rho(1 + G_1)}{Q} \frac{r}{\xi} \frac{d\xi}{dr}}_{(6)} + \underbrace{k^2 \left(P_\parallel - \frac{B^2}{2} \right)}_{(7)} \right.$$

$$\left. \underbrace{- \frac{\rho\lambda(1 - G_2) + \rho\lambda \frac{\omega k}{\omega_{ci}} r(1 + G_1)}{Q}}_{(8)} \right]_{r^-}^{r^+} , \qquad (9) \qquad (68)$$

where r^- and r^+ are to the inside and to the outside of the layer. We define

$$\kappa^\pm = \mp \frac{1}{\xi} \frac{d\xi(r^\pm)}{dr} , \qquad (69)$$

where $\kappa^{\pm} = |k|$ is accurate if ω/kV_A, $1/kR$, $1/k(r_w - R) \ll 1$, with r_w the wall radius and R the location of the layer's center, the latter to be identified as the average radius of (unfavorable) curvature in our z-pinch model. Simple scaling allows us to neglect the following terms in Eq. (68):

$$\text{Term (1)} \ll \text{Term (6)}, \text{ if } k\Delta \ll 1;$$

$$\text{Term (8)} \ll \text{Term (6)}, \text{ if } 1/kR \ll 1; \text{ and}$$

$$\text{Term (5)} \ll \text{Term (9)}, \text{ if } \Delta \ll \Delta_b.$$

Further, we note that the pressure at r^- is just the background pressure since the location of r^- is chosen so that the hot electron annulus pressure is negligible there.

1. Background Plasma Interchange Layer Mode

First, we look at very low frequency modes where $\omega \ll kV_A$, ω_{ci}, $\omega_{cv\perp}$, which allows us to neglect terms (2) and (9) in Eq. (68). Hence we evaluate the G terms in the limit $\omega \to 0$. For simplicity, we neglect β compared with unity and take $G_2 = G_3 = 0$. Therefore, in Eq. (68),

$$1 + G_1 = -\left(\frac{r}{B}\frac{dB}{dr}\right)^{-1}\left(1 + \frac{r}{B^2}\frac{dP_{\perp c}}{dr}\right). \tag{70}$$

Note that if a finite $P_{\parallel h}$ were to be included, the essential form would instead be

$$1 + G_1 \approx -\left(\frac{rdB}{Bdr}\right)^{-1}\left(1 + \frac{P_{\parallel h}}{P_{\perp h}} + \frac{r}{B^2}\frac{dP_{\perp c}}{dr}\right) . \qquad (71)$$

Then, in Eq. (68), we are left with terms (4), (6), and (7), which yield the equation

$$-\int_{r^-}^{r^+} dr \frac{k^2}{\left(1 + \frac{r}{B^2}\frac{dP_{\perp c}}{dr}\right)} \frac{d}{dr}\left(\frac{B^2}{2}\right)$$

$$= -\omega^2 \rho(r^-) R\kappa^- - k^2 P_{\parallel c}(r^-) + \frac{k^2}{2}\left[B^2(r^-) - B^2(r^+)\right] . \qquad (72)$$

This equation reduces to

$$\omega^2 = \frac{k^2}{\rho(r^-)\kappa^- R}\left[-P_{\parallel c}(r^-) - \int_{r-}^{r^+} dr \frac{\frac{r}{B}\frac{dP_{\perp c}}{dr}\frac{dB}{dr}}{\left(1 + \frac{r}{B^2}\frac{dP_{\perp c}}{dr}\right)}\right]$$

$$\approx \frac{|k|}{R\rho(r^-)}\left\{\frac{\left[P_{\perp c}(r^-)\overline{\frac{r}{B}\frac{dB}{dr}}\right]}{1 + \frac{R}{B^2}\frac{dP_{\perp c}}{dr}} - P_{\parallel c}(r^-)\right\} , \qquad (73)$$

where $\kappa^- \approx |k|$ and where we assume $-(1/P_{\perp c})[dP_{\perp c}(r)/dr] \simeq 1/\Delta$ on the outer half of the annulus and $(-1/P_{\perp c})dP_{\perp c}/dr << 1/\Delta$ on the inner half of the annulus. The term $\overline{r/B(dB/dr)}$ is evaluated by averaging over only the outer half of the annulus. If $-(R/B^2)(dP_{\perp c}/dr) << 1$, we see that this mode is stable when $(R/B)(dB/dr) > 1$. This is a stable flute interchange. However, when $-(R/B^2)(dP_{\perp c}/dr) > 1$ [with parallel

pressure, the criterion is $-R\left(dP_{\perp c}/dr\right)/B^2 > 1 - \left(dP_{\parallel c}/dr\right)/\left(B\ dB/dr\right)$, the background plasma beta instability threshold of Refs. 7 and 8 is surpassed and this mode is unstable.

Near this critical beta threshold, we need to keep frequency-dependent terms in the expression for G_1 to avoid a divergence. Doing so, we find that the dispersion relation becomes

$$\omega^2 = \frac{|k|}{R\rho(r^-)} \left[-P_{\parallel c}(r^-) + \int_{r^-}^{r^+} dr \frac{\left(1 - \varepsilon - \frac{\omega^2 r}{k^2 V_A^2 B}\frac{dB}{dr}\right)\frac{d}{dr}\left(\frac{B^2}{2}\right) - \frac{\omega}{\omega_{cv\perp}}\frac{d}{dr}\left(P_{\perp h} + P_{\perp c}\right)}{\varepsilon - \frac{\omega}{\omega_{cv\perp}} + \frac{\omega^2}{k^2 V_A^2}\frac{r}{B}\frac{dB}{dr}} \right] \tag{74}$$

with $\varepsilon = 1 + \left(dP_{\perp c}/dr\right)r/B^2$. We assume that the interesting response occurs when

$$1 \gg \varepsilon, \frac{\omega}{\omega_{cv\perp}}, \frac{\omega^2}{k^2 V_A^2}\left(\frac{r}{B}\right)\frac{dB}{dr} .$$

We then need only include the unity term in the numerator of the integrand in Eq. (74). If we further assume that ε is constant on the outer half of the layer and $dP_{\perp c}/dr$ negligible on the inner half and also that

$$\omega \ll \frac{\left(\frac{rdB}{Bdr}\right)^{-1} k^2 V_A^2}{\omega_{cv\perp}} ,$$

we can integrate Eq. (74) and obtain

$$\omega^2 = \frac{|k| B^2 \Delta/\Delta_b}{R\rho(r^-)(\varepsilon - \omega/\omega_{cv\perp})} . \qquad (75)$$

In Eq. (75), the $P_{\parallel c}$ term has been dropped for simplicity. Also, for the layer modes, we have defined the fractional change of the magnetic field strength from outside to within the hot electron annulus layer as $[B^2(r^+) - B^2(R)]/2B^2(R) = \Delta/\Delta_b$. We then find the instability criterion to be

$$\varepsilon < \varepsilon_{cr} = \frac{3}{4^{1/3}} \left[\frac{|k| B^2 \Delta/\Delta_b}{R\rho(r^-)\omega_{cv\perp}^2}\right]^{1/3} , \qquad (76)$$

with the growth rate, $Im(\omega)$, maximized at $\varepsilon = 0$, where its value is

$$Im(\omega) = \frac{\sqrt{3}}{2} \left(\frac{V_A^2 |k| \Delta\omega_{cv\perp}}{R\Delta_b}\right)^{1/3} , \qquad (77)$$

with $V_A^2 = B^2(R)/\rho(r^-)$.

The self-consistency of our assumptions for this marginal analysis requires

$$1 > \left(\frac{k^2 V_A^4}{\Delta_b^2 \omega_{cv\perp}^4} \frac{\Delta^2}{R^2} \right) > \frac{1}{(k\Delta_b)^3} \left(\frac{\Delta}{\Delta_b} \right)^3 . \qquad (78)$$

The left-hand inequality in Eq. (78) arises from the assumption $\varepsilon_{cr} << 1$, and the right-hand inequality arises from the assumption $\omega << k^2 V_A^2 \Delta_b / R\omega_{cv\perp}$. We will not consider the violation of the right-hand inequality as it is incompatible with subsequent stability criteria that will be discussed, if $\beta_h^2 < k\Delta$.

However, if the left-hand inequality of Eq. (78) is violated, that is, if $|k| V_A^2 (\Delta/\Delta_b R) >> \omega_{cv\perp}^2$, the threshold for instability can be reduced. If in this limit we assume $\varepsilon \simeq 1$, then integrating Eq. (74) across the annulus yields (in the integral we neglect terms proportional to $\omega^2/k^2 V_A^2$)

$$\omega^2 = \frac{|k| V_A^2}{\Delta_b} \frac{\Delta \delta_c''}{R} \frac{\left(1 + \frac{\omega}{\bar{\omega}_{cv\perp}} \frac{\Delta_b}{R} \right)}{\left(1 - \frac{\omega}{\bar{\omega}_{cv\perp}} \right)} , \qquad (79)$$

where $\delta_c'' = -R(dP_{\perp c}/dr)/B^2$ and where terms proportional to $\omega^2/k^2 V_A^2$ have been neglected in the integral. Assuming $\Delta_b/r << 1$, we then find the stability requirement to be

$$-\frac{R}{B^2}\frac{dP_{\perp c}}{dr} < \frac{4}{27}\left|\frac{\omega_{cv\perp}^2 R\Delta_b}{|k|V_A^2\Delta}\right| \equiv \delta''_{cr} \quad . \tag{80}$$

Substantially above this reduced threshold, when $\delta''_c >> R^3\delta''_{cr}/\Delta_b^3$, but still below the critical beta threshold of Eq. (76), the growth rate is that of an interchange mode due to the background pressure only:

$$\gamma = \left\{\frac{|k|}{R\rho(r^-)}\left[P_{\perp c}(r^-) + P_{\parallel c}(r^-)\right]\right\}^{1/2}, \tag{81}$$

where we have included the contribution from the $P_{\parallel c}$ term in Eq. (74).

2. Compressional Layer Mode

Another solution to Eq. (68) is associated with a zero of the denominator Q. Let us define ω_0 such that

$$Q(\omega_0, r_0) = 0 \quad , \tag{82}$$

$$\frac{\partial}{\partial r} Q(\omega_0, r_0) = 0 \quad . \tag{83}$$

We shall show that in fact the eigenfrequency can be ω_0 for thin annuli. The demonstration follows from keeping terms (2), (4), (5), and (6) in Eq. (68) and then expanding about ω_0 and r_0, using $\omega' \equiv \omega - \omega_0$, and $r' \equiv r - r_0$. If we are at marginal stability $(\partial Q/\partial\omega_0 = 0)$, then Eq. (68) becomes

$$-\lambda R\rho(r^-)\,|k| \approx \int_{r^-}^{r^+} \frac{dr' \left[\frac{-\omega_0^2}{\omega_{ci}^2}\left(\frac{\lambda^2 \rho r_0}{V_A^2}\right) + \frac{k^2 B^2}{r_0} + \frac{2\omega_0}{\omega_{ci}}\,\lambda\rho k \right]}{\frac{r'^2}{2}\,\frac{\partial^2 Q}{\partial r^2}\left(\omega_0, r_0\right) + \frac{\omega'^2}{2}\,\frac{\partial^2 Q}{\partial \omega^2}\left(\omega_0, r_0\right)} \tag{84}$$

Assuming that the integral in Eq. (84) is peaked at $r = r_0$, we evaluate the numerator at r_0 and find

$$\left(\frac{\omega'}{\omega_0}\right)^2 = \frac{4\pi^2}{\omega_0 \frac{\partial^2 Q}{\partial r^2}\frac{\partial^2 Q}{\partial \omega^2}\left[k\lambda r_0 \rho(r^-)\right]^2}\left[\frac{\omega_0^2}{\omega_{ci}^2}\frac{\lambda^2 \rho(r_0) r_0}{V_A^2(r_0)} + \frac{k^2 B_0^2}{r_0} + \frac{2\omega_0}{\omega_{ci}}\,\lambda\rho k\right]^2 . \tag{85}$$

From dimensional scaling we have

$$\frac{\partial^2 Q}{\partial r^2} \sim \frac{Q}{\Delta^2}, \qquad \frac{\partial^2 Q}{\partial \omega^2} \sim \frac{Q}{\omega_0^2},$$

$$Q \sim \frac{\Delta_b}{r}, \qquad \lambda \sim \frac{k^2 V_A^2 \Delta_b}{r},$$

so that

$$\left(\frac{\omega'}{\omega_0}\right)^2 \sim 4\pi^2 k^2 \Delta^2 \left(\left|\frac{\omega_0^2}{\omega_{ci}^2}\right|, \frac{1}{k^2 \Delta_b^2}, \frac{2\omega_0}{\omega_{ci} k \Delta_b} \right)^2 , \tag{86}$$

which vanishes as $k\Delta \to 0$ (but with Δ_b/R finite). However, because of the large coefficients, the requirement that ω'/ω_0 be small can

become a stringent condition on the subsequent analysis, for realistic physical parameters.

Now, to consider Eqs. (82) and (83) in more detail, we take a model where

$$P_h = \frac{P_{h0}}{(1 + r'^2/\Delta^2)} \tag{87}$$

$$P_c = \begin{cases} P_{c0} , & r' < 0 \\ \dfrac{P_{c0}}{(1 + r'^2/\Delta^2)} , & r' > 0 . \end{cases} \tag{88}$$

Here, $P_h = P_{\perp h}$ since the parallel hot electron pressure is zero, and the background pressure P_c is taken to be isotropic.

If we assume that $B' = B(r_0 + r') - B(r_0)$, the change of the magnetic field strength, is small compared to $B_0 \equiv B(r_0)$, the equilibrium condition can be written as

$$B'B_0 + P_\perp = -r' \frac{B_0^2}{r_0} , \tag{89}$$

with $P_\perp = P_h + P_c$. Therefore

$$B' = -B_0\left[\frac{r'}{r_0} + \frac{P_0}{B_0^2}\frac{1}{(1 + r'^2/\Delta^2)}\right], \qquad r' > 0 \ , \qquad (90)$$

where $P_0 = P_{c0} + P_{h0}$.

Equations (82) and (83) in normalized form then reduce to

$$Q(y,x) = \frac{y - 1 + \delta_c \dfrac{x}{(1 + x^2)^2}}{y - 1 + \delta \dfrac{x}{(1 + x^2)^2}} - \frac{y^2}{\left(1 - \dfrac{y^2}{y_{ci}^2}\right)} \frac{1}{(1 + x^2)\kappa^2} = 0 \ , \qquad (91)$$

$$\frac{\partial}{\partial x} Q(y,x) \propto -\frac{\delta(1 - 3x^2)}{(y - 1)(1 + x^2)^2 + x\delta} + \frac{\delta_c(1 - 3x^2)}{(y - 1)(1 + x^2)^2 + x\delta_c} + 2x$$

$$= 0 \ , \qquad (92)$$

with

$$\delta = \frac{2P_{h0}r_0}{\Delta B^2}, \qquad \delta_c = \frac{2P_{c0}r_0}{\Delta B^2},$$

$$y = \frac{\omega}{\omega_{cv\perp}}, \qquad y_{ci} = \frac{\omega_{ci}}{\omega_{cv\perp}},$$

$$x = \frac{r'}{\Delta}, \qquad \kappa^2 = \frac{k^2 B_0^2}{\rho_0 \omega_{cv\perp}^2} \ ,$$

where we have chosen $\rho(x) = \rho_0/(1 + x^2)$. Numerical solutions of

Eqs. (91) and (92) for marginal stability are given in Figs. 2(a) and 2(b) for $\delta_c = 0$ and .5, respectively, and for various values of δ. The stable region is generally above the curves (for low background ion density), although for sufficiently small δ it is possible to have stability below the curves (for high background density).

The general structure of Figs. 2(a) and (b) can be explained analytically if we take $\delta_c << 1$ and assume $(y - 1)\left(1 + x^2\right)^2 < \delta x$. Then Eqs. (91) and (92) are satisfied for $x^2 = 1/5$, and we need to consider the dispersion relation

$$Q\left(y, \frac{1}{\sqrt{5}}\right) = \frac{(y - 1)}{y - 1 + .31\delta} - \frac{.83y^2}{\left(1 - \frac{y^2}{y_{ci}^2}\right)\kappa^2} = 0 \quad . \qquad (93)$$

The validity of the assumption $(y - 1) < \delta x$ requires either $\delta >> 1$ or $\kappa^2 >> 1$. The latter condition is satisfied at marginal stability when $y_{ci} \simeq 1$. We see that this mode is unstable with too much density. The density threshold is very low when $y_{ci} \simeq 1$, and there is no density threshold when $y_{ci} = 1$. However, as was already mentioned, the validity of our layer analysis is marginal near $y_{ci} = 1$, and for this case a more sophisticated theory is needed to obtain a realistic threshold density.

If $\delta >> 1$, the stability criteria obtained from analyzing the cubic dispersion relation, Eq. (93), are given by

$$\frac{V_A^2}{V_{cv\perp}^2} > \delta \qquad \text{if} \quad y_{ci} >> 1, \tag{94}$$

$$\frac{V_A^2}{V_{cv\perp}^2} > \frac{1}{4}\delta \left(y_{ci}\right)^2 \qquad \text{if} \quad y_{ci} << 1, \tag{95}$$

and

$$\frac{V_A^2}{V_{cv\perp}^2} > \frac{\frac{1}{2}\delta}{\left(y_{ci} - 1\right)^2} \qquad \text{if} \quad y_{ci} \approx 1 \ , \tag{96}$$

where $V_{cv\perp} = \omega_{cv\perp}/k$ and $V_A^2 = B_0^2/\rho_0$.

If δ is not too large, it is also possible to have stability at high ion density. This can be seen analytically by solving Eq. (93) in the limit when $y << 1$ and $\kappa << y_{ci}$, namely,

$$y^3 - ay^3 + \kappa^2/.83 = 0 \ , \tag{97}$$

with $a = 1 - .31\delta$. The roots of Eq. (97) are stable if

$$\kappa^2 < .13a^3 \ . \tag{98}$$

Thus, as long as $\delta < 3.23$, there can exist a stable region at high density, as indicated in Fig. 2.

B. WKB-Type Modes

The second type of modes to consider are short wavelength ones that can be described by WKB analysis, where d/dr is replaced by ik_r. As a rough guide we will use the quantitization rule $k_r\Delta \simeq (n + \nu_n)\pi$. In Appendix B we show that $\nu_0\pi \simeq 2$ for a special model and for a particular mode. For simplicity of presentation we will take $\nu_0 = 2/\pi$ in the quantitative calculations that follow. Using the particular results given in Eqs. (63) - (65) for a delta function distribution and with the background pressure taken to be isotropic, the local dispersion relation for Eq. (39) is

$$k_\perp^2(1 + G_1) - \frac{\omega^2}{V_A^2}$$

$$+ \frac{k^2V_A^2}{\lambda R}\left[\left(1 + G_1 - \frac{\lambda}{k^2V_A^2}\right)\left(\frac{P_\parallel}{B^2\Delta} + \frac{1}{\Delta_b} - \frac{3}{2}\frac{\beta_c}{R}\right) + \frac{(1 - \beta_c/2)^2}{R}\right]$$

$$+ \frac{2\omega}{\omega_{ci}}\frac{k(1 - \beta_c/2)}{R} - \frac{(1 - \beta_c/2)}{\Delta R} - \frac{\omega}{\omega_{ci}}\frac{k}{\Delta}(1 + G_1) = 0 \ , \qquad (99)$$

where R is the radius of curvature, $\Delta = -P/(dP/dr) = -\rho/(d\rho/dr)$, and

$$1 + G_1 = \frac{\omega(1 + \hat{\beta}) - \omega_{cv\perp}\left[1 - \frac{R}{\Delta}\frac{P_c}{B^2}\left(1 + \frac{2\Delta}{\Delta_b}\right)\right]}{\omega - \omega_b} \qquad (100)$$

with

$$\hat{\beta} = \beta - \frac{\beta_h \mu_0 B}{2\gamma_0 m_e c^2} \quad . \tag{101}$$

Equation (99) can be expressed as a fifth-order polynomial in the normalized frequency $y = \omega/\omega_{cv\perp}$:

$$y^5 + Ay^4 + By^3 + Cy^2 + Dy + E = 0 \quad , \tag{102}$$

with

$$A = -\frac{\omega_b}{\omega_{cv\perp}} + \frac{k(1+\hat{\beta})V_A^2}{\omega_{ci}\Delta\omega_{cv\perp}} - \frac{2kV_A^2(1-\beta_c/2)}{\omega_{ci}\omega_{cv\perp}R} \approx \tilde{\beta} - 1 + \frac{p}{\tilde{\beta}_h}\left(\frac{R}{\Delta}\right)^2 \tag{103}$$

$$B = -\frac{k_\perp^2 V_A^2(1+\hat{\beta})}{\omega_{cv\perp}^2} - \frac{V_A^2 k\left(g + \frac{2\Delta}{\Delta_b}(1-\beta_c/2)\right)}{\omega_{ci}\Delta\omega_{cv\perp}}$$

$$+ \frac{V_A^2}{R\Delta\omega_{cv\perp}^2}\left(1 - \beta_c/2 + \frac{\Delta}{\Delta_b}\eta\right)$$

$$+ \frac{k^2 V_A^4}{\omega_{cv\perp}^2\omega_{ci}^2 R\Delta_b}\left[\eta(1+\hat{\beta}) + \frac{\Delta_b}{R}\left(1 - \beta_c/2\right)^2\right]$$

$$\approx -\frac{p}{\tilde{\beta}_h}\left(\frac{R}{\Delta}\right)^2\left[1 + \frac{1}{q} - \tilde{\beta}_c - p\left(1 + \frac{2\tilde{\beta}_c}{\tilde{\beta}_h}\right)\right] \tag{104}$$

$$C = \frac{gk_\perp^2 V_A^2}{\omega_{cv\perp}^2} + \frac{V_A^2(1-\beta_c/2)}{\Delta\Delta_b\omega_{cv\perp}^2} + \frac{\eta V_A^2}{\Delta_b^2\omega_{cv\perp}^2} + \frac{k^2 V_A^4 \beta_c \Gamma}{2\omega_{cv\perp}^2\omega_{ci}^2\Delta_b\Delta}$$

$$\approx \frac{p}{q\tilde{\beta}_h}\left(\frac{R}{\Delta}\right)^2\left[1 - \tilde{\beta}_c + p\tilde{\beta}_c q\left(1 + \frac{2\tilde{\beta}_c}{\tilde{\beta}_h} - \frac{2}{\tilde{\beta}_h}\right)\right] \tag{105}$$

$$D = -\frac{k^2 V_A^4}{\omega_{cv\perp}^4 R\Delta_b}\left[\eta(1 + \hat{\beta}) + \frac{\Delta_b}{R}(1 - \beta_c/2)^2\right]$$

$$\approx -\left(\tilde{\beta}_h + 2\tilde{\beta}_c\right)\left(\frac{pR}{q_0 k_\perp^2 \Delta^2 \tilde{\beta}_h}\right)^2 \tag{106}$$

$$E = -\frac{k^2 V_A^4 \Gamma \beta_c}{2\Delta_b \Delta \omega_{cv\perp}^4}$$

$$\approx -\left(\frac{R}{\Delta}\right)\left(\frac{\tilde{\beta}_c}{\tilde{\beta}_h}\right)\left(\frac{p}{q_0 k\Delta}\right)^2\left(1 + \frac{2\tilde{\beta}_c}{\tilde{\beta}_h} - \frac{2}{\tilde{\beta}_h}\right) \tag{107}$$

We have defined the following quantities:

$$p = \frac{n_h}{n_c} \tag{108}$$

$$q = \frac{k^2 V_{cv\perp}}{k_\perp^2 \omega_{ci}\Delta} = \left(\frac{k}{k_\perp}\right)^2 q_0 \tag{109}$$

$$\tilde{\beta} = \beta\left(\frac{R}{2\Delta}\right) = \tilde{\beta}_c + \tilde{\beta}_h \tag{110}$$

$$g = 1 - \frac{R}{\Delta}\frac{\beta_c}{2}\left(1 + \frac{2\Delta}{\Delta_b}\right) \approx 1 - \tilde{\beta}_c \tag{111}$$

$$\eta = 1 + \frac{\beta_c \Delta_b}{2\Delta} - \frac{3}{2}\beta_c \frac{\Delta_b}{R} \approx \frac{\tilde{\beta}_h + 2\tilde{\beta}_c - 1}{\tilde{\beta}_h + \tilde{\beta}_c - 1} \tag{112}$$

$$\Gamma = \left(1 + \frac{2\Delta}{\Delta_b}\right)\eta - \left(1 - \frac{3\Delta}{R}\right)\frac{\Delta_b}{R} - 2\left(1 - \beta_c/4\right)\frac{\Delta}{R}$$

$$\simeq \frac{\tilde{\beta}_h + 2\tilde{\beta}_c - 2}{\tilde{\beta}_h + \tilde{\beta}_c - 1} . \qquad (113)$$

In the approximate forms of coefficients A - E of Eqs. (103) - (107), and also in the approximate forms of Eqs. (111) - (113), we have neglected terms of order $\beta_{c,h}$ and Δ/R compared to unity and used the relationship $n_h = (m_e\gamma_0/\mu_0 B)P_h$ derivable from Eq. (62). We will assume $\beta R/\Delta \sim 0(1)$ and therefore use these approximate forms in the analytical investigation of the modes of Eq. (102) that follows.

1. High Frequency Modes

To study the modes with frequencies $\omega > \omega_{ci}$, we keep only the A, B, and C terms in Eq. (102) and justify this procedure a posteriori. Well above threshold when $y^2 \simeq -C/A$, we find the compressional magnetic instability, $\omega^2 = -k_\perp^2 V_A^2(1 - \tilde{\beta}_c)/(\tilde{\beta}_h - 1)$, in the limit $p < 2\tilde{\beta}_h(\Delta/R)^2$, and the high-frequency hot electron interchange instability, $\omega^2 = -\omega_{ci}^2 q_0(k_\perp\Delta)^2$, when $p = 1$ and $q_0 >> 1$. The marginal stability condition for these modes is $B^2 = 4AC$, which can be written as

$$p\left\{p^2\left(1+\frac{2\tilde{\beta}_c}{\tilde{\beta}_h}\right)^2 - 2p\left[\left(1+\frac{1}{q}+\tilde{\beta}_c\right)\left(1+\frac{2\tilde{\beta}_c}{\tilde{\beta}_h}\right) - \frac{4\tilde{\beta}_c}{\tilde{\beta}_h}\right] + \left(1-\frac{1}{q}-\tilde{\beta}_c\right)^2\right\}$$

$$= 4\left(\frac{\Delta}{R}\right)^2\left(\tilde{\beta}-1\right)\tilde{\beta}_h\left[p\tilde{\beta}_c\left(1+\frac{2\tilde{\beta}_c}{\tilde{\beta}_h}-\frac{2}{\tilde{\beta}_h}\right)+\frac{1}{q}\left(1-\tilde{\beta}_c\right)\right]. \quad (114)$$

As a cubic equation in p, Eq. (114) generally has two roots near $p \simeq 1$ and another at very small $p \lesssim (\Delta/R)^2 << 1$. However, the larger of the two roots near unity is spurious, being always greater than unity, whereas physically the hot electron density may not exceed the ion density. We now analyze Eq. (114) in these two limits.

a. High-frequency Hot Electron Interchange.

For this case, we take $p \sim 1$ and thus neglect the right-hand side of Eq. (114), obtaining a quadratic equation in p. There is one physical solution (i.e., with $p \leq 1$), which leads to an upper limit on p for stability:

$$p < p_1 \equiv \left[1-\left(\frac{1}{q}+\tilde{\beta}_c\right)^{1/2}\right]^2. \quad (115)$$

Equation (115) is therefore the stability condition for the high-frequency ($\omega > \omega_{ci}$) version of the hot electron interchange mode.[5] Notice, however, that for small values of q as specified by

$$q < \left(4 - \tilde{\beta}_c\right)^{-1} \longrightarrow \frac{1}{4} \qquad \text{if } \tilde{\beta}_c << 1 \ , \tag{116}$$

p_1 exceeds unity and then this mode is stable.

b. Compressional Mode.

For the $p << 1$ case, we analyze Eq. (114) as a linear equation, neglecting the p^3 and p^2 terms. The small root p_2 provides a lower bound for stability:

$$p > p_2 \equiv \frac{1}{q}\left(\frac{2\Delta}{R}\right)^2 \tilde{\beta}_h \left(\tilde{\beta} - 1\right)\left(1 - \tilde{\beta}_c\right)\left(1 - \frac{1}{q} - \tilde{\beta}_c\right)^{-2} . \tag{117}$$

Equation (117) is the stability condition for the new compressional magnetic mode.[12,13] It shows that at negligible $\tilde{\beta}_c$, instability can arise with too much background plasma. It also shows that when $\tilde{\beta}_c \approx 1$, the root p_2 vanishes and this mode is stable. Hence, associated with the compressional mode are both a density and a beta condition. Only the latter was obtained from the energy principle analysis.[9]

c. Disappearance of Stability

The assumptions employed in deriving the stability criteria of Eqs. (115) and (117) for the two high-frequency modes fail when $s \equiv 1 - q^{-1} - \tilde{\beta}_c \approx 0$. The root p_1 minimizes at zero when $s = 0$, while p_2 becomes large. Therefore, when s is sufficiently small,

the roots p_1 and p_2 can coalesce, with the result that stability disappears altogether.

We can analyze this case by solving Eq. (114) with the assumption $p \sim s^2 << 1$. Thus, neglecting the p^3 term, Eq. (114) becomes a quadratic,

$$p^2 - \frac{1}{4}s^2 p + \left(\frac{\Delta}{R}\right)^2 d^2 \left(\tilde{\beta} - 1\right) = 0 \quad , \tag{118}$$

with $s << d \equiv 1 - \tilde{\beta}_c$. Equation (118) shows that no real roots for p are possible, corresponding to the coalescence of p_1 and p_2 and the nonexistence of stability, when

$$s^4 \equiv \left(1 - \frac{1}{q} - \tilde{\beta}_c\right)^4 < 64 \left(\frac{\Delta}{R}\right)^2 \tilde{\beta}_h \left(\tilde{\beta} - 1\right)\left(1 - \tilde{\beta}_c\right)^3 \quad . \tag{119}$$

Note that Eq. (119) is quantitatively accurate only for small hot electron beta values $(\beta_h < .25)$. Nonetheless, we conclude from this analysis that a region in wavenumber space exists for which there is no stability. A similar conclusion has also been reached by El Nadi.[13] However, since this intrinsically unstable region is somewhat narrow in parameter space, we expect that more realistic geometrical effects need to be taken into account for an accurate application of this theory to the current experiments, where stable operation has been empirically determined.

Finally, dimensional analysis of Eq. (102) establishes that our high-frequency analysis which has kept only the A, B, and C terms is generally accurate if $k^2 p_1/q\left(k_\perp^2\Delta\right)^2 \ll 1$. This is not a serious restriction on the analysis, although the marginal stability condition for the high-frequency hot electron interchange mode near $q = 1/4$ must be somewhat modified if $k/k_\perp^2\Delta \sim 1$.

2. Low-frequency Hot Electron Interchange

To study the conventional ($\omega < \omega_{ci}$) hot electron interchange mode,[3,4] we consider the B, C, and D terms of Eq. (102). By dimensional arguments, one can show that this procedure is justified if $q \ll 1$ and $\beta_c \ll \beta_h$. The typical growth rate for this mode well above threshold is given by $\omega^2 = -\omega_{cv\perp}^2 p/q_0\left(k_\perp\Delta\right)^2 = -\omega_{ci}^2 pq$. The stability condition for this mode, $C^2 \leq 4BD$, yields another upper limit on the density ratio p:

$$p < p_3 \equiv \frac{1}{4}\left(k_\perp\Delta\right)^2 q_0 \left(1 - \tilde{\beta}_c\right)^2 . \qquad (120)$$

3. Low-frequency Background Plasma Interchange

In order to investigate the background plasma pressure-driven interchange modes, we retain terms B, C, D, and also E in Eq. (102). The dispersion relation can then be written (for $p \ll 1$) as

$$[1 + q(1 - \tilde{\beta}_c)]y^3 - (1 - \tilde{\beta}_c)y^2 + \tau\left(1 + \frac{2\tilde{\beta}_c}{\tilde{\beta}_h}\right)y$$

$$+ \tau\tilde{\beta}_c\left(1 + \frac{2\tilde{\beta}_c}{\tilde{\beta}_h} - \frac{2}{\tilde{\beta}_h}\right) = 0 \quad , \tag{121}$$

with $\tau = p/q_0(k_\perp\Delta)^2$. Observe that $\tau < 1$ is essentially the condition for the low-frequency hot electron interchange mode to be stable (when $\tilde{\beta}_c << 1$) . In the following analysis, we will assume $\tau << 1$.

The well-known growth rate above threshold for the background plasma interchange instability is obtained from $y^2 = -E/C$ as

$$\omega^2 = -\left(\frac{k}{k_\perp}\right)^2\left(\frac{V_A^2\beta_c}{R\Delta}\right)\frac{(1 - \tilde{\beta}_h/2 - \tilde{\beta}_c)}{(1 - \tilde{\beta}_c)} \quad . \tag{122}$$

The expression of Eq. (122) follows from treating the hot electrons as rigid and non-interacting, and it is valid for $\tilde{\beta}_c << 1$. We will first analyze the stability for this case and then consider the case where the background plasma interacts with a non-rigid hot electron annulus.

a. Non-interacting Background Interchange $(\beta_c << 2\Delta/R)$

In this case, we analyze the pure background interchange mode, with stability determined only by terms C, D, and E in Eq. (102).

It can be seen that there are two possibilities for achieving stability. If the hot electrons create a sufficiently deep diamagnetic well according to

$$\beta_h > \frac{4\Delta}{R} - 2\beta_c \quad , \tag{123}$$

intrinsic stability can be obtained. However, even if Eq. (123) is not satisfied, stability can still be achieved if

$$\tau > 4\tilde{\beta}_c \left(1 - \tilde{\beta}_c\right) \left(\frac{2}{\tilde{\beta}_h} - 1 - \frac{2\tilde{\beta}_c}{\tilde{\beta}_h}\right) \left(1 + \frac{2\tilde{\beta}_c}{\tilde{\beta}_h}\right)^{-2}$$

$$\longrightarrow 8\left(\frac{\beta_c}{\beta_h}\right) \quad \text{if} \quad \tilde{\beta}_h >> 1 \quad \text{and} \quad \beta_c/\beta_h < 1 \; . \tag{124}$$

This latter stabilization mechanism arises from the difference in density between the ions, n_c, and the electrons, n_e, of the background plasma, the difference being the hot electron density. Thus, since $n_c \neq n_e$, the ion $\underset{\sim}{E}\times\underset{\sim}{B}$ rotational drift is not completely cancelled to lowest order. This results in a frequency shift proportional to $(n_c - n_e)/n_c = p$ for the interchange mode, which, in

a manner analogous to finite Larmor radius stabilization,[17] produces stability if $\tau \propto p$ is large enough, as specified by Eq. (124).

b. Interacting Background Interchange $(\beta_c \sim 2\Delta/R)$

In the situation when $\tilde{\beta}_c \simeq 1$, we must analyze the cubic equation, (121). We may drop the linear term under the assumption $\tau << d^2/3$, with $d = 1 - \tilde{\beta}_c$ again. For small d, two roots of the cubic dispersion relation coalesce and lead to instability if

$$d \equiv 1 - \tilde{\beta}_c < 3\left[\frac{\tau}{4}\left(1 + \frac{2\tilde{\beta}_c}{\tilde{\beta}_h} - \frac{2}{\tilde{\beta}_h}\right)\right]^{1/3} . \qquad (125)$$

The maximum growth rate occurs when $d = 0$ and is given by

$$\mathrm{Im}(\omega) = \frac{\sqrt{3}}{2}\,\omega_{cv\perp}\left[\tau\left(1 + \frac{2\tilde{\beta}_c}{\tilde{\beta}_h} - \frac{2}{\tilde{\beta}_h}\right)\right]^{1/3} . \qquad (126)$$

4. Numerical Solutions

In Figs. 3 and 4, we present a set of detailed plots of the marginal stability boundaries of the short-wavelength WKB modes described by Eq. (102). The stability criteria are a mixture of density and beta limits. Thus, Figs. 3 and 4 are dual plots of the background ion density n_c and the background plasma beta β_c as functions of the hot electron density n_h and beta β_h, for fixed temperatures.

The values for β and Δ/R in these numerical plots are arbitrary, that is, not restricted to having values small compared to unity.

Fig. 3 is for EBT-S parameters: B = 5 kG, Δ = 1 cm, R = 20 cm, r_p = 10 cm where r_p is the experimental annulus radius, the relativistic hot electron energy is $(\gamma - 1)m_e c^2$ = 500 eV, $\beta_c = n_c T_{ec}$, T_{ec} = 200 eV where we note that the electron temperature is then equal to $T_{ec} n_c/(n_c - n_h)$, which for most parameters is essentially T_{ec}. Figs. 3(a) - 3(f) are for various values of the poloidal mode number $m = kr_p$ (m = 1,3,6,8,12, and 20). For these parameters, the quantity $q_0 = 7.6$, with $q = .019m^2/(1 + 2.5\times10^{-3}m^2)$.

To interpret Fig. 3(a) for m = 1, for which $q << 1$, we observe that the lower ion density bound for the hot electron interchange mode given by Eq. (120) is satisfied. For EBT-S parameters, in fact, Eq. (120) will be satisfied for all m values, and hence the lower frequency hot electron instability is not excited. We also note that for very small q, the upper n_c density limit of Eq. (117) for the compressional mode is always satisfied. Hence the upper stability limit is the critical background beta criterion[7,8] given by

$$\beta_c < \left(\frac{2\Delta}{R}\right)\left[1 - \beta_h + \frac{2\Delta}{R}\left(1 + \frac{\beta_h}{2}\right)\right]\left(1 + \frac{2\Delta}{R}\right)^{-1}, \qquad (127)$$

where we have included small corrections of $O(\beta)$ and $O(\Delta/R)$ in the analytic result of Eq. (127). The left-hand stability boundary in Fig. 3(a) is given by Eqs. (123) and (124). In the upper part of this left-hand boundary, the quantity τ is negligible compared to unity and

the stability condition can be approximated by the deep diamagnetic well condition on β_h given by Eq. (123). At lower background density, τ is larger and stabilization can be achieved for smaller β_h in accordance with Eq. (124).

In Fig. 3(b), for $m = 3$ (where $q = .17$), we observe the stability boundary associated with the compressional mode, which is given by the inequality of Eq. (117). For fixed background temperature, this condition has two roots for the background density, one where $\beta_c R/2\Delta \simeq 1$ and one for $\beta_c R/2\Delta \ll 1$. Hence, in Fig. 3(b), there is an additional band of instability where the lower curve is the density threshold for the compressional mode, whereas the upper part of the instability band shows that the compressional mode stabilizes as the critical background beta limit of Eq. (127) is approached.

Fig. 3(c) presents the stability plot for $m = 6$, where $q = .68$. In this case the small region of stability near the critical β_c limit is not resolved in the figure. The lower ion density band of stability is now determined below by the high-frequency hot electron interchange given by Eq. (115) and above by the compressional mode of Eq. (117). In Fig. 3(d) for $m = 8$ (where $q = 1.05$), we see that this island of stability has disappeared, in accordance with Eq. (119). For higher m values, a stability window reappears, as shown in Figs. 3(e) and 3(f) for $m = 12$ and $m = 20$, respectively.

Figure 4 exhibits stability plots for parameters corresponding to the proof-of-principle EBT-P device: B = 10 kG, Δ = 1.5 cm, R = 26 cm, r_p = 18 cm, $(\gamma - 1)m_e c^2$ = 1 Mev, and T_{ec} = 2 keV . For these EBT-P parameters, $q = 3.0\times10^{-3}m^2/[1 + 1.7\times10^{-3}m^2]$. Figures 4(a) - 4(e) are for m = 1,15,20,35, and 60, respectively.

In Fig. 4(a), the upper boundary for stability is the critical β_c limit of Eq. (127), and the left-hand boundary is given by Eq. (124). The lower boundary is the physical constraint $n_c = n_h$ for small hot electron beta values, since the stability condition for the conventional hot electron interchange, Eq. (120), is satisfied. However, for $\beta_h > .6$, the low-frequency hot electron interchange mode determines the lower ion density stability boundary. The stability picture is similar for m = 15 (where q = .49) in Fig. 4(b), except that the lower density stability boundary now arises from the high-frequency hot electron interchange condition given by Eq. (115).

In Fig. 4(c), the stability boundary for m = 20 is shown (q = .71). In this case, the new band of instability is due to the density limit given by Eq. (117), with the two roots being present as discussed in Fig. 3(b). In Fig. 4(d) for m = 35, where q = 1.19 , the stability window has disappeared in accordance with Eq. (119). A very thin stability region exists just below the critical β_c limit of Eq. (127). In Fig. 4(e) for m = 60 (q = 1.52), stability reappears.

For the EBT-P parameters chosen in Fig. 4, we have $q_0 = 1.8$; therefore, a wide band of wavenumbers can satisfy Eq. (119), resulting in instability. This feature is observed when one compares the results shown in Figs. 4(a) - 4(e) with those in Figs. 3(a) - 3(f).

V. SUMMARY OF RESULTS

We have developed a self-consistent theory for the curvature-driven instabilities of a hot electron plasma in a z-pinch model. One can apply the results of this theory to a bumpy torus if one associates (a) the radius of the annulus in our z-pinch model with the average radius of curvature of the magnetic field sampled by the hot electrons and (b) the wavenumber k in the z-direction of symmetry with the poloidal wavenumber m/r_p, where m is an integer and r_p is the experimentally measured minor radial position of the hot electrons with respect to the magnetic axis.

The stability picture that emerges is as follows.

If the dynamics of the hot electrons can decouple from those of the background plasma, and if the hot electron beta, β_h, is sufficiently large so that

$$\beta_h \geq \frac{4\Delta}{R} - 2\beta_c \quad , \tag{128}$$

where Δ is the hot electron annulus half-width, R the radius of curvature, and β_c the background plasma beta, then the hot electrons create a diamagnetic well that stably confines the background plasma. Generally, the conditions for the decoupling of the hot electron dynamics are that:

(1) The background ion density , n_c ,be sufficiently high so that the ideal MHD growth rate for the low-frequency hot electron interchange is sufficiently less than the curvature drift frequency (calculated using the perpendicular energy) and also that the high-frequency hot electron interchange mode not be excited;

(2) The background density be sufficiently low so that, roughly, the curvature drift frequency is less than the compressional Alfvén frequency; and

(3) The background plasma beta, β_c, be sufficiently low, namely, $\beta_c \lesssim 2\Delta/R$.

Conditions (1) and (2) indicate that a window in the values of the background plasma density for stable operation may be present. Condition (3) sets a limit on the background plasma beta that can be contained. These conditions need to be studied carefully when a complete survey of parameters is considered, particularly the finite ion cyclotron frequency. There then arises a range of parameters where the stability window can disappear. To improve on the stability picture at these parameters, it will be necessary both to solve our radial eigenmode equation more accurately and to introduce additional physics, such as the axial variation of equilibrium quantities and the effects of finite Larmor radius. We leave the study of these effects to a subsequent investigation.

To be more quantitative, we note that we have found two types of modes: (a) short-wavelength WKB-like modes where a substantial fraction of a radial wavelength, $2\pi/k_r$, fits across the outer edge of the hot electron annulus of half-thickness Δ (somewhat arbitrarily we have chosen $k_r\Delta = 2$, which is the longest wavelength for one particular model); and (b) layer modes whose radial wavelengths are long compared to the annulus thickness.

For the short wavelength modes, even when $\beta_h > 4\Delta/R - 2\beta_c$, four other types of curvature-driven instabilities were found:

(1) A low-frequency ($\omega < \omega_{ci}$) hot electron instability. This instability is driven by the hot electron pressure and is predictable from MHD theory. It is stabilized if the hot electron to background ion density fraction satisfies

$$\frac{n_h}{n_c} < \frac{k_\perp^2 \Delta^2}{4} q_o \left(1 - \frac{\beta_c R}{2\Delta}\right)^2 , \qquad (129)$$

where R is the radius of curvature, $k_\perp^2 = k_r^2 + k^2$, $q_0 = V_{cv\perp}/\omega_{ci}\Delta = (\gamma^2 - 1)c^2/(2\gamma\omega_{ce}\omega_{ci}R\Delta)$, $\gamma m_e c^2$ is the mean relativistic energy of the electrons, β_c the background plasma beta, and $\omega_{ce,i}$ the electron and ion cyclotron frequencies (in units of radians/sec). Since $q_0 > 1$ in present EBT experiments, this criterion is readily satisfied. For reactor-like devices, however, this criterion becomes quite significant.

(2) A high-frequency hot electron instability that is driven by the hot electron pressure when frequencies are comparable or greater than the ion cyclotron frequency. To excite this instability one generally needs

$$q \equiv \frac{k^2}{k_\perp^2} q_0 > \frac{1}{4} . \tag{130}$$

Stabilization is achieved if

$$\frac{n_h}{n_c} < \left[\left(1 - \frac{1}{q} + \frac{\beta_c R}{2\Delta}\right)^{1/2}\right]^2 . \tag{131}$$

This is not a stringent criterion as long as $q \neq 1/(1 - \beta_c R/2\Delta)$. However, when $q \simeq 1/(1 - \beta_c R/2\Delta)$, the above condition goes to zero, indicating that there is no stable value for n_h/n_c. However, this result probably depends on our idealization of the mathematical model. A calculation incorporating more realistic physical effects is needed.

(3) A compressional Alfvén instability is excited if the background plasma ion density , n_c , is too large. The stability condition requires

$$\frac{n_h}{n_c} > \frac{2\beta_h \Delta q}{R} \frac{\left(\frac{R\beta}{2\Delta} - 1\right)\left(1 - \frac{\beta_c R}{2\Delta}\right)}{\left[1 - q\left(1 - \frac{\beta_c R}{2\Delta}\right)\right]^2} , \tag{132}$$

where β_h is the hot electron beta. This condition gives a reasonable upper density limit if $q \neq 1/(1 - \beta_c R/2\Delta)$. However, when $q \simeq 1/(1 - \beta_c R/2\Delta)$, the above condition has no stable operating region. In fact, when $q \simeq 1/(1 - \beta_c R/2\Delta)$, the compressional Alfvén and high-frequency hot electron modes coalesce, and analysis then shows that there is no stable operating regime (assuming $\beta_c R/2\Delta \ll 1$) when

$$\left(1 - \frac{1}{q}\right)^4 < 32 \frac{\beta_h \Delta}{R} \left(\frac{R\beta}{2\Delta} - 1\right) . \qquad (133)$$

[Eq. (133) requires $\beta_h < .25$ for its validity.] We note that if $q_0 < 1$, we can avoid this unstable region. If $q_0 \gg 1$, only a relatively narrow band of parameters is resonant, and the introduction of additional effects may yield reasonable stability properties. However, if $q_0 \simeq 1$, we conjecture that even more realistic modeling will have difficulty in finding stable operation.

(4) A background pressure-driven mode arises when $\beta_c R/2\Delta > 1$, which is the basic background beta limit discussed by Van Dam and Lee[7] and Nelson.[8] At fixed background temperature, this condition also limits the background density. In order that this background beta limit be the governing limit for stability, rather than the density limit of the compressional Alfvén mode, we require

$$\frac{T_c}{T_h} > \left(\frac{4\Delta}{R}\right) \beta_h q_0 \qquad \text{for } q_0 \ll 1 . \qquad (134)$$

If, for $q_0 \gg 1$, we assume that a more realistic theory will spread

the denominator of Eq. (132) so that it has a minimum value of order unity, then the condition of Eq. (134) is altered to

$$\frac{T_c}{T_h} > T\left(\frac{\Delta}{R}\right)\beta_h\left(1 - \frac{2\Delta}{R\beta_h}\right) \quad \text{for} \quad q_0 >> 1 , \qquad (135)$$

where T is a number of order unity.

For the long-wavelength layer modes, we do not find the hot electron pressure-driven interchange modes, since the hot electron pressure has no net change across the annulus layer. We still find background density limits due to the compressional Alfvén-type mode. If $k\Delta q_0 << 1$, the stability limit for this mode is similar to Eq. (132) with $q = q_0$, viz.,

$$\frac{n_h}{n_c} > \frac{\beta_h^2}{2} q_0 , \qquad (136)$$

where we have assumed $R\beta/2\Delta >> 1$ and $\beta_c R/2\Delta << 1$. For $k\Delta q_0 >> 1$, the stability condition becomes

$$\frac{n_h}{n_c} > \frac{\beta_h^2}{q_0(k\Delta)^2} . \qquad (137)$$

However for $k\Delta q_0 \to 1$, we find that there is no stability region. Here too, more realistic calculations are needed. In particular, the

condition for justifying the layer approach breaks down when $\omega_{ci} = kv_{cv\perp}$.

We find that the long-wavelength background pressure-driven interchange layer mode is also limited by the condition $\beta_c < 2\Delta/R$. However, for some parameters the background beta limit can be substantially less. For example, using Eq. (80), we have

$$\beta_c < \beta_{crit} \equiv \frac{2\Delta}{R} \text{Min}\left[1, \frac{4k\Delta q_0}{27\left(1 - \frac{2\Delta}{R\beta_h}\right)\frac{n_h}{n_c}}\right]$$

$$\simeq \frac{2\Delta}{R} \text{Min}\left[1, \frac{4k\Delta}{27\left(1 - \frac{2\Delta}{R\beta_h}\right)\beta_h^2}\right] , \qquad (138)$$

where we have bounded n_h/n_c by Eq. (136) and assumed $q_0 << 1$. Thus, since $k\Delta$ can be as small since Δ/r, the critical β_c limit can be reduced below $2\Delta/R$, as β_h increases to moderate values that are still less than unity.

Acknowledgements

The authors have benefited from fruitful discussions with A. El-Nadi.

This work was supported by the Office of Fusion Energy, OER, United States Department of Energy, under contract DE-FG05-80ET-53088 with the University of Texas and under contract W-7405-eng-26 with the Union Carbide Corporation and also by the University of Texas Program Development Fund.

APPENDIX A

Derivation of the Parallel Current Equation

By using the identities

$$\underset{\sim}{J}\times\underset{\sim}{B} = -\underset{\sim}{\nabla}\left(\frac{B^2}{2}\right) + \underset{\sim}{B}\cdot\underset{\sim}{\nabla}\underset{\sim}{B} \quad , \tag{A.1}$$

$$\underset{\sim}{\nabla}\cdot\underset{\sim}{\underset{\sim}{P}} = \underset{\sim}{\nabla}P_\perp + \underset{\sim}{B}\underset{\sim}{B}\cdot\underset{\sim}{\nabla}\left(\frac{P_\parallel - P_\perp}{B^2}\right) + \left(\frac{P_\parallel - P_\perp}{B^2}\right)\underset{\sim}{B}\cdot\underset{\sim}{\nabla}\underset{\sim}{B} \quad , \tag{A.2}$$

which follow simply from the Maxwell equations $\underset{\sim}{J} = \underset{\sim}{\nabla}\times\underset{\sim}{B}$ and $\underset{\sim}{\nabla}\cdot\underset{\sim}{B} = 0$, and by assuming a diagonal pressure tensor of the form $\underset{\sim}{\underset{\sim}{P}} = P_\parallel\hat{\underset{\sim}{b}}\hat{\underset{\sim}{b}} + P_\perp(\underset{\sim}{\underset{\sim}{I}} - \hat{\underset{\sim}{b}}\hat{\underset{\sim}{b}})$ with $\hat{\underset{\sim}{b}} = \underset{\sim}{B}/|B|$, we can rewrite the momentum equation $\rho\dot{\underset{\sim}{V}} = \underset{\sim}{J}\times\underset{\sim}{B} - \underset{\sim}{\nabla}\cdot\underset{\sim}{\underset{\sim}{P}}$ as

$$\rho\dot{\underset{\sim}{V}} = -\underset{\sim}{\nabla}\left(\frac{B^2}{2} + P_\perp\right) + \sigma\underset{\sim}{B}\cdot\underset{\sim}{\nabla}\underset{\sim}{B} + \underset{\sim}{B}\underset{\sim}{B}\cdot\underset{\sim}{\nabla}\sigma \quad , \tag{A.3}$$

with $\dot{\underset{\sim}{V}} = d\underset{\sim}{V}/dt$ and $\sigma = 1 + (P_\perp - P_\parallel)/B^2$. Our objective now is to calculate the component along $\underset{\sim}{B}$ of the curl of the momentum equation, (A.3).

First, we operate on the right-hand side of Eq. (A.3):

$$\underset{\sim}{B}\cdot\underset{\sim}{\nabla}\times\left[-\nabla\left(\frac{B^2}{2} + P_\perp\right) + \sigma\underset{\sim}{B}\cdot\underset{\sim}{\nabla}\underset{\sim}{B} + \underset{\sim}{B}\underset{\sim}{B}\cdot\underset{\sim}{\nabla}\sigma\right]$$

$$= \underset{\sim}{B}\cdot\underset{\sim}{\nabla}\times\left[\sigma(\underset{\sim}{J}\times\underset{\sim}{B}) + (\sigma - 1)\underset{\sim}{\nabla}\left(\frac{B^2}{2}\right) + \underset{\sim}{B}\underset{\sim}{B}\cdot\underset{\sim}{\nabla}\sigma\right] \quad . \tag{A.4}$$

Consider the various terms individually:

$$\underset{\sim}{B}\cdot\underset{\sim}{\nabla}\times\left[\sigma(\underset{\sim}{J}\times\underset{\sim}{B})\right] =$$

$$-2\sigma\underset{\sim}{J}\cdot(\underset{\sim}{B}\cdot\underset{\sim}{\nabla}\underset{\sim}{B}) + \underset{\sim}{B}\cdot\underset{\sim}{\nabla}(\sigma\underset{\sim}{J}\cdot\underset{\sim}{B}) - B^2(\underset{\sim}{J}\cdot\underset{\sim}{\nabla}\sigma) - \sigma B^2(\underset{\sim}{\nabla}\cdot\underset{\sim}{J}), \qquad (A.5)$$

where the last term in Eq. (A.5) may be dropped by charge neutrality ($\nabla\cdot\underset{\sim}{J} = 0$);

$$\underset{\sim}{B}\cdot\underset{\sim}{\nabla}\times\left[(\sigma - 1)\,\underset{\sim}{\nabla}\left(\frac{B^2}{2}\right)\right] = (\underset{\sim}{B}\times\underset{\sim}{\nabla}\sigma)\cdot\underset{\sim}{\nabla}\left(\frac{B^2}{2}\right) \quad ; \qquad (A.6)$$

and

$$\underset{\sim}{B}\cdot\underset{\sim}{\nabla}\times(\underset{\sim}{B}\underset{\sim}{B}\cdot\underset{\sim}{\nabla}\sigma) = (\underset{\sim}{B}\cdot\underset{\sim}{J})(\underset{\sim}{B}\cdot\underset{\sim}{\nabla}\sigma) \quad . \qquad (A.7)$$

Therefore, the right-hand side of Eq. (A.4) contributes the following:

$$\underset{\sim}{B}\cdot\underset{\sim}{\nabla}\times\left[-\underset{\sim}{\nabla}\left(\frac{B^2}{2} + P_\perp\right) + \sigma\underset{\sim}{B}\cdot\underset{\sim}{\nabla}\underset{\sim}{B} + \underset{\sim}{B}\underset{\sim}{B}\cdot\underset{\sim}{\nabla}\sigma\right]$$

$$= B^2\underset{\sim}{B}\cdot\underset{\sim}{\nabla}\left(\frac{\sigma\underset{\sim}{J}\cdot\underset{\sim}{B}}{B^2}\right) - (\underset{\sim}{B}\times\underset{\sim}{\kappa})\cdot\underset{\sim}{\nabla}\left(B^2 + P_\perp - P_\parallel\right). \qquad (A.8)$$

where $\underset{\sim}{\kappa} = \hat{\underset{\sim}{b}}\cdot\underset{\sim}{\nabla}\hat{\underset{\sim}{b}} = [\underset{\sim}{B}\cdot\underset{\sim}{\nabla}\underset{\sim}{B} - \hat{\underset{\sim}{b}}\hat{\underset{\sim}{b}}\cdot\nabla\,(B^2/2)]/B^2$ is the magnetic field line curvature.

Operating on the left-hand side of Eq. (A.3) produces

$$\underset{\sim}{B}\cdot\underset{\sim}{\nabla}\times\rho\dot{\underset{\sim}{V}} = \underset{\sim}{\nabla}\cdot(\rho\dot{\underset{\sim}{V}}\times\underset{\sim}{B}) + \rho\dot{\underset{\sim}{V}}\cdot\underset{\sim}{J} \quad . \qquad (A.9)$$

We shall assume that the ion motion is transverse to the magnetic field, i.e., $\dot{\underset{\sim}{V}} = \dot{\underset{\sim}{V}}_{\perp}$.

Finally, use Eq. (A.3) to rewrite one of the terms in Eq. (A.8), viz.,

$$(\underset{\sim}{B}\times\underset{\sim}{K})\cdot\underset{\sim}{\nabla}\left(B^2 + P_{\perp} - P_{\parallel}\right) =$$

$$(\underset{\sim}{B}\times\underset{\sim}{K})\cdot\underset{\sim}{\nabla}\left(\frac{B^2}{2} - P_{\parallel}\right) - \rho\dot{\underset{\sim}{V}}\cdot\underset{\sim}{J}_{\perp} - \rho\dot{\underset{\sim}{V}}\cdot(\hat{\underset{\sim}{b}}\times\underset{\sim}{\nabla}B). \qquad (A.10)$$

Combining Eqs. (A.8), (A.9), and (A.10) yields the desired result:

$$\underset{\sim}{\nabla}\cdot(\underset{\sim}{B}\times\rho\dot{\underset{\sim}{V}}) + B^2\underset{\sim}{B}\cdot\underset{\sim}{\nabla}\left(\frac{\sigma\underset{\sim}{J}\cdot\underset{\sim}{B}}{B^2}\right) - (\underset{\sim}{B}\times\underset{\sim}{K})\cdot\underset{\sim}{\nabla}\left(\frac{B^2}{2} - P_{\parallel}\right)$$

$$+ \rho\dot{\underset{\sim}{V}}\cdot(\hat{\underset{\sim}{b}}\times\underset{\sim}{\nabla}B) = 0. \qquad (A.11)$$

APPENDIX B

Model Radial Calculation

To estimate $k_r\Delta$, we consider the following model. Define $r' = r - R$ (where R is the annulus radius in our z-pinch model and also the radius of field-line curvature) and choose

$$\frac{1}{B}\frac{dB}{dr} = \begin{cases} -1/R\ , & r' < -\Delta \\ -1/\Delta_b\ , & -\Delta < r' < 0 \\ 1/\Delta_b\ , & 0 < r' < \Delta \\ -1/R\ , & r' > \Delta \end{cases} \qquad \text{(B.1)}$$

$$\rho = \begin{cases} \rho_0\ , & r' < 0 \\ \rho_0\left(1 - \frac{r'}{\Delta}\right)\ , & 0 < r' < \Delta \\ 0, & r' > 0\ . \end{cases} \qquad \text{(B.2)}$$

Furthermore, we assume the change in $B(r')$ to be small relative to B, take $R >> \Delta_b$, and assume $\omega_{ci}^2 << k^2 V_A^2$, $\omega << \omega_{cv\perp}$, $\omega >> \omega_{ci}$, and $k << k_\perp$. We will describe the Alfvén compressional instability. With $Q \simeq 1 + G_1 = -B/(R\ dB/dr)$, the relevant terms of the governing differential equation [Eq. (39)] are

$$\frac{d}{dr}\left(\rho \frac{d\xi}{dr}\right) - \frac{\omega^2 \rho^2}{B^2}\left(\frac{R\frac{dB}{dr}}{B}\right) \xi = 0 . \qquad (B.3)$$

The local dispersion relation in the outer part of the layer for $\gamma = -i\omega$ at $r' = 0$ is

$$\gamma = k_r V_A \left(\frac{B}{R\frac{dB}{dr}}\right)^{1/2} = \frac{k_r B}{\rho_0^{1/2}} \left(\frac{\Delta_b}{R}\right)^{1/2} . \qquad (B.4)$$

We wish to determine the eigenvalue of the spatially varying problem in order to estimate k_r.

Using the profiles in Eqs. (B.1) and (B.2) and defining $x = r'/\Delta$, we find that Eq. (B.3) becomes

$$\frac{d}{dx}(1 - x) \frac{d\xi^+}{dx} + \frac{R\Delta^2}{\Delta_b V_{A0}^2} \gamma^2 (1 - x)^2 \xi^+ = 0, \qquad 0 < x < 1 \qquad (B.5)$$

$$\frac{d^2}{dx^2}(\xi^-) - \frac{R}{\Delta_b} \frac{\Delta^2 \gamma^2}{V_{A0}^2} \xi^- = 0 , \qquad -1 < x < 0 , \qquad (B.6)$$

where $V_{A0}^2 = B^2/\rho_0$.

Assuming $\Gamma_0 \equiv \left[(R\Delta^2\gamma^2/(\Delta_b V_{A0}^2)\right]^{1/2}$ is reasonably larger than unity, the solution for ξ^- is

$$\xi^- = A \exp(\Gamma_0 x) . \qquad (B.7)$$

The nonsingular solution for ξ^+ is a Bessel function:

$$\xi^+ = J_0\left[\frac{2}{3}\Gamma_0\left(1-x\right)^{3/2}\right] . \qquad \text{(B.8)}$$

The eigenvalue is determined by equating logarithmic derivatives of ξ^+ and ξ^- at $x = 0$, which yields

$$1 = \frac{-J_0'}{J_0} = \frac{J_1}{J_0} . \qquad \text{(B.9)}$$

where J_0' represents the derivative of J_0 with respect to the entire argument. The solution to Eq. (B.9) for the lowest mode is $2\Gamma/3 \simeq 1.4$, or

$$\gamma \simeq 2\frac{V_{A0}}{\Delta}\left(\frac{\Delta_b}{R}\right)^{1/2} . \qquad \text{(B.10)}$$

Comparing Eqs. (B.10) with (B.4) yields

$$k_r\Delta \simeq 2 . \qquad \text{(B.11)}$$

References

1. R. A. Dandl, H. O. Eason, P. H. Edmonds, and A. C. England, Nucl. Fusion 11, 411 (1971).

2. H. Ikegami, H. Ikezi, M. Hosokawa, S. Tanaka, and K. Takayama, Phys. Rev. Lett. 19, 779 (1967).

3. N. A. Krall, Phys. Fluids 9, 820 (1966).

4. H. L. Berk, Phys. Fluids 19, 1255 (1976).

5. R. R. Dominguez and H. L. Berk, Phys. Fluids 21, 827 (1978).

6. D. B. Nelson, Nucl. Fusion 19, 283 (1979).

7. J. W. Van Dam and Y. C. Lee, in Proc. EBT Ring Physics Workshop (ORNL, Oak Ridge, 1979), Conf-791228, p. 471.

8. D. B. Nelson, Phys. Fluids 23, 1850 (1980).

9. J. W. Van Dam, M. N. Rosenbluth, and Y. C. Lee, Institute for Fusion Studies Report-12, (1981), University of Texas at Austin, to be published in Phys. Fluids.

10. T. M. Antonsen, B. Lane and J. J. Ramos, Phys. Fluids 24, 1465 (1981).

11. D. M. Kruskal and C. Oberman, Phys. Fluids 1, 275 (1958).

12. D. A. Spong and A. M. El Nadi, Bull. Am. Phys. Soc. 25, 964 (1980).

13. A. M. El Nadi, to be published in Phys. Fluids.

14. H. L. Berk, M. N. Rosenbluth, and J. W. Van Dam, in Proceedings of U. S.--Japan Workshop on Non-Axisymmetric Confinement Systems", Institute for Fusion Studies Report-5 (1980), University of Texas at Austin.

15. M. N. Rosenbluth, Phys. Rev. Lett. 46, 1525 (1981).

16. J. W. Van Dam, H. L. Berk, M. N. Rosenbluth, and D. A. Spong, in Proc. EBT Stability Theory Workshop (ORNL, Oak Ridge, 1981), Conf-810512, p. 97; D. A. Spong, J. W. Van Dam, H. L. Berk, and M. N. Rosenbluth, op cit, p. 15.

17. M. N. Rosenbluth, N. A. Krall, and N. Rostoker, Nucl. Fusion, Suppl. Part 1, 143 (1962).

Figure Captions

Fig. 1. Z-pinch model for a hot electron plasma: Hot electrons are located in the shaded annular region, with background plasma existing in the region occupied and enclosed by the annulus. Magnetic field is in the $-\hat{\theta}$ direction.

Fig. 2. Marginal stability curves for the compressional layer mode, with δ as the parameter for each curve and for the two cases of (a) $\delta_c = 0$ and (b) $\delta_c = 0.5$.

Fig. 3. Marginal stability curves for the short-wavelength WKB modes, calculated using EBT-S parameters for various mode number values.

Fig. 4. Marginal stability curves for the short-wavelength WKB modes, calculated using EBT-P parameters for various mode numbers.

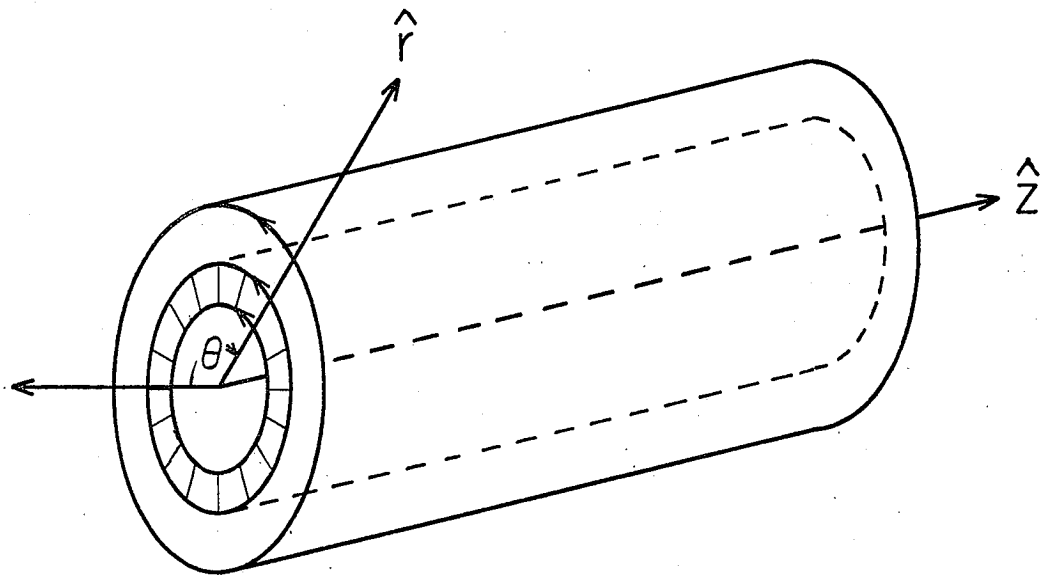

Fig. 1

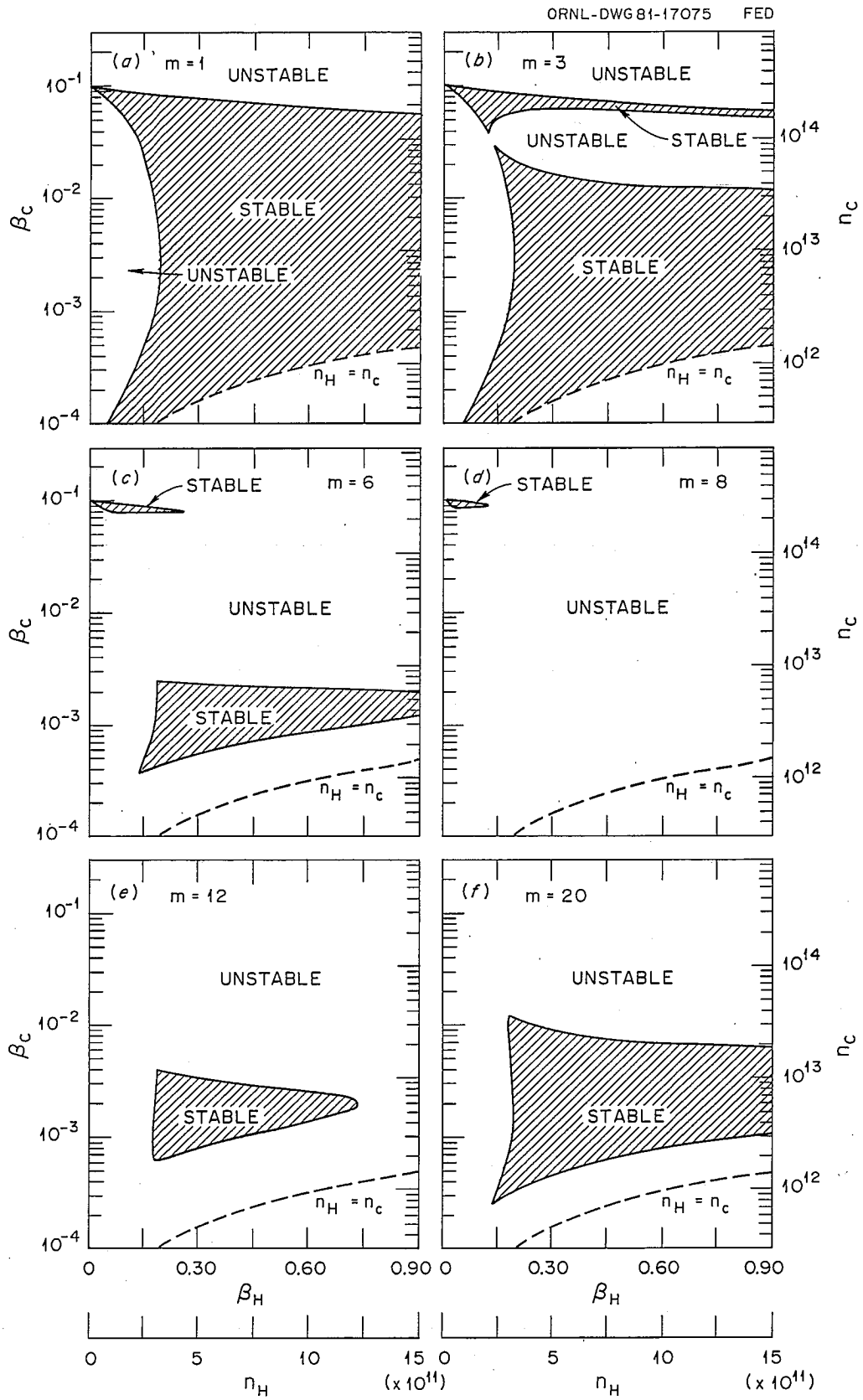
ORNL-DWG 81-17075 FED
(a) m = 1
UNSTABLE
STABLE
UNSTABLE
$n_H = n_c$
(b) m = 3
UNSTABLE
UNSTABLE
STABLE
STABLE
$n_H = n_c$
(c) STABLE
m = 6
UNSTABLE
STABLE
$n_H = n_c$
(d) STABLE
m = 8
UNSTABLE
$n_H = n_c$
(e) m = 12
UNSTABLE
STABLE
$n_H = n_c$
(f) m = 20
UNSTABLE
STABLE
$n_H = n_c$
β_c
n_c
10^{-1}
10^{-2}
10^{-3}
10^{-4}
10^{14}
10^{13}
10^{12}
0
0.30
0.60
0.90
β_H
0
5
10
15
n_H
$(\times 10^{11})$

Fig. 2

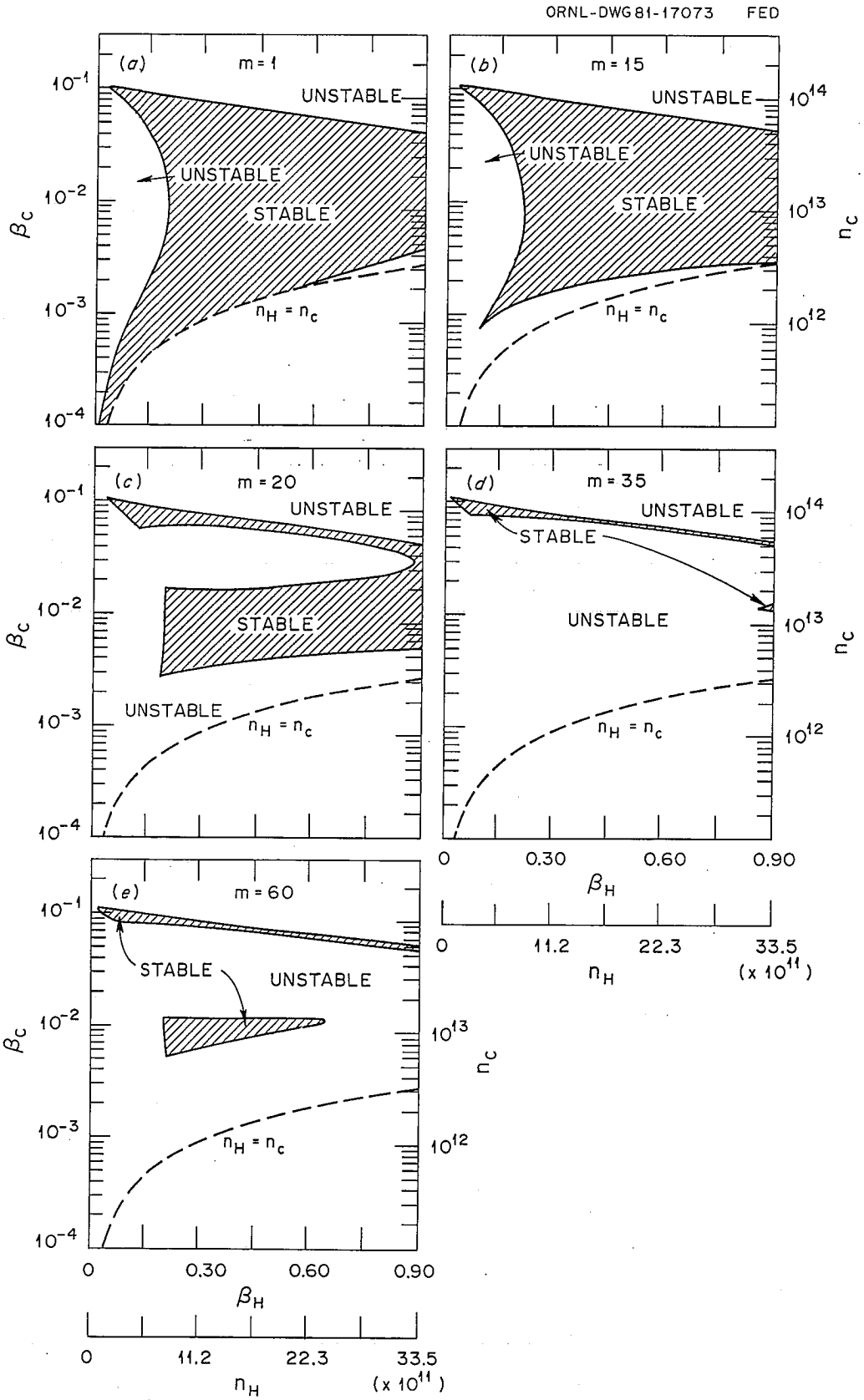
ORNL-DWG 81-17073 FED
(a) m = 1
UNSTABLE
UNSTABLE
STABLE
$n_H = n_c$
(b) m = 15
UNSTABLE
UNSTABLE
STABLE
$n_H = n_c$
(c) m = 20
UNSTABLE
STABLE
UNSTABLE
$n_H = n_c$
(d) m = 35
UNSTABLE
STABLE
UNSTABLE
$n_H = n_c$
(e) m = 60
STABLE
UNSTABLE
$n_H = n_c$
β_c
10^{-1}
10^{-2}
10^{-3}
10^{-4}
n_c
10^{14}
10^{13}
10^{12}
0
0.30
0.60
0.90
β_H
0
11.2
22.3
33.5
(x 10^{11})
n_H

Fig. 3